Optimal Therapy Scheduling Based on a Pair of Collaterally Sensitive Drugs

Nara Yoon, Robert Vander Velde, Andriy Marusyk and Jacob G. Scott

October 13, 2017

Abstract

Despite major strides in the treatment of cancer, the development of drug resistance remains a major hurdle. To address this issue, researchers have proposed sequential drug therapies with which the resistance developed by a previous drug can be relieved by the next one, a concept called collateral sensitivity. The optimal times of these switches, however, remains unknown.

We therefore developed a dynamical model and study the effect of sequential therapy on heterogeneous tumors comprised of resistant and sensitivity cells. A pair of drugs ($DrugA$, $DrugB$) are utilized and switched in turn within the therapy schedule. Assuming that they are collaterally sensitive to each other, we classified cancer cells into two groups, and explored their population dynamics: A_R and B_R, each of which is subpopulation of cells resistant to the indicated drug and concurrently sensitive to the other.

Based on a system of ordinary differential equations for A_R and B_R, we determined that the optimal treatment strategy consists of two stages: initial stage in which a chosen better drug is utilised until a specific time point, T, and afterward; a combination of the two drugs with relative durations (i.e. $f\Delta t$-long for $DrugA$ and $(1-f)\Delta t$-long for $DrugB$ with $0 \leq f \leq 1$ and $\Delta t \geq 0$). Of note, we prove that the initial period, in which the first drug is administered, T, is shorter than the period in which it remains effective in lowing total population, contrary to current clinical intuition.

We further analyzed the relationship between population makeup, $ApB = A_R/B_R$, and effect of each drug. We determine a specific makeup, ApB^*, at which the two drugs are equally effective. While the optimal strategy is applied, ApB is changing monotonically to ApB^* and then remains at ApB^* thereafter.

Beyond our analytic results, we explored an individual based stochastic model and presented the distribution of extinction times for the classes of solutions found. Taken together, our results suggest opportunities to improve therapy scheduling in clinical oncology.

1 Introduction

Drug resistance is observed in many patients after exposure to cancer therapy, and is a major hurdle in the cancer therapy [1]. Treatment with appropriate chemo- or targeted therapy reliably reduces tumor burden upon initiation. However, resistance inevitably arises, and disease burden relapse [2]. The disease recurrence is visible, at the earliest, when disease burden reaches a threshold of detection, at which first therapy is considered failed and a second line drug is used, to control the disease

in more efficient way (see Figure 1 (a)). Redesign of treatment is required to start earlier than the time point, not only because the detection threshold is higher than the minimum disease burden, but also because first drug could become less efficient as duration of therapy reaches to T_{max}. In this research, we focus on the latter reason and figure out how much earlier we should switch drug in advance of T_{max}, assuming that the former reason is less important ($t_{DT} - t_o \approx T_{max}$).

In preexisting tumor, both resistant and sensitive types of cells against a therapy are thought to co-exist even before the beginning of the therapy [3], and the cellular composition is shaped according to choices of drugs (diagrammed at Figure 1 (b)). Such alteration of cell populations is toward gaining resistant properties against the drug being administered, due to (i) kinetic changes affecting DNA synthesize during S-phase [4], (ii) drug induced genetic (point) mutations [5], or (iii) phenotypic plasticity and resulting epigenetic modifications [6].

To deal with the resistance developed by a drug, one can prescribe a different drug as a follow-up therapy targeting the resistance issue. Researchers have sought specific combinations that induce sensitivity, this is the concept of collateral sensitivity [7, 8, 9]. In specific cases, an order of several drugs complete a collateral sensitivity cycle [8], and corresponding periodic drug sequence can be used in prescription of a long term therapy – though we recently showed that the continued efficacy of the same cycle is not guaranteed [10]. In this research, we focused on such drug cycling comprised by just two drugs, each of which can be used as a targeted therapy treating non-cross resistant factors occurring after the therapy of the other drug (diagrammed on Figure 1 (b)).

(a) Drug resistance

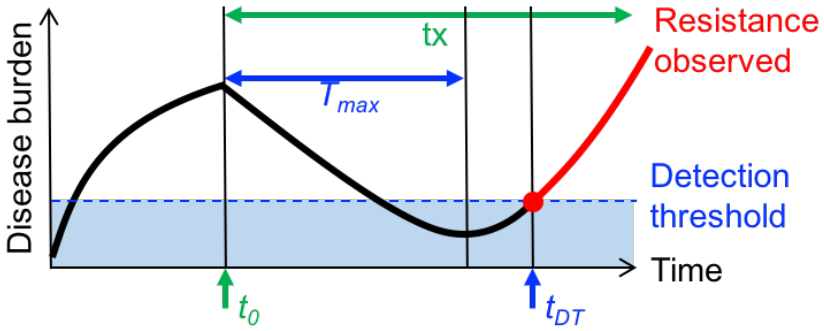

(b) Tumor heterogeneity and collateral sensitivity

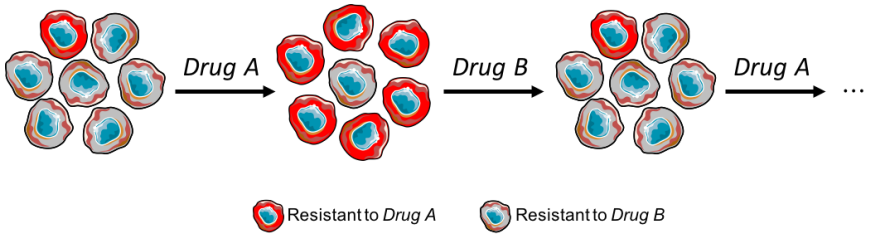

Figure 1: (a) General dynamical pattern of disease burden. It increases initially and then decreases as of the therapy starting point (t_0), and eventually rebounds after the maximum period with positive therapy effect (T_{max}). Relapse is found, at the earliest, when disease burden reaches detection threshold at t_{DT}. (b) Change in composition of tumor cell population when a pair of collaterally sensitive drugs are given one after another.

The underlying dynamics of resistance development has been studied by looking cell popula-

tions mixed by sensitive and resistant types against therapy/therapies, whether it is genotypic or phenotypic classifications [11]. Additionally, many researchers have accounted for their choices of detailed cellular heterogeneities like: (i) stages in evolutionary structures [12, 13], (ii) phases of cell cycle [14, 15, 16, 17], or (iii) spatial distribution of irregular therapy effect [18, 19]. Among them, many researches (including [11, 15, 16, 20, 21]) studied the effect of a pair of non-cross resistant drugs like us, using the Goldie-Coldman model or its variations [12, 21, 22, 23]. Those models are basically utilizing population structure of four compartments each of which represents subpopulation (i) sensitive to the both drugs, (ii) and (iii) resistant to one of them respectively, or (iv) resistant to both.

In this research, we want to propose a simpler modeling structure including only two types of subpopulations (see Section 2 for the detail), which is still appropriate in the study of collaterally sensitive drug effect and whose simplicity facilitates mathematical derivations of interesting concepts and quantities (see Section 3 for the detail of the analytical derivations). The model we propose at Section 2 has a potential to be expanded with other important considerations as well, like comparable stochastic simulations described in Section 4 and other future works explained in Section 5.

2 Modeling setup

2.1 Basic cell population dynamics under a single drug administration

Before describing the comprehensive model for collateral sensitive network in Section 2.2, let us go over a fundamental modeling structure describing dynamical behavior of cell populations under a single drug. Based on the sensitivity and resistance to the therapy, cell population can be split into two groups. Then, we call the populations of the sensitive cells and the resistant cells by C_S and C_R respectively, and use total cell population, $C_P = C_S + C_R$, in measuring disease burden and drug effect.

We account three dynamical events in our model: proliferation of sensitive (s) and resistant cells (r), and transition between the cell types (g). Here, net proliferation rate represents combined birth and death rate, so can be positive if birth rate is higher than death rate or negative otherwise. It is reasonable to assume that, under the presence of drug, sensitive cell population declines ($s < 0$), resistant cell population increases ($r > 0$), and $g > 0$ for transition.

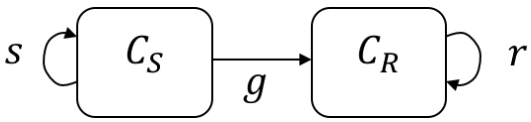

$$\begin{pmatrix} \dot{C}_S \\ \dot{C}_R \end{pmatrix} = \begin{pmatrix} -(g-s) & 0 \\ g & r \end{pmatrix} \begin{pmatrix} C_S \\ C_R \end{pmatrix} \quad (1)$$

Figure 2: Diagram of dynamics between sensitive cells population, C_S, and resistant cells population, C_R, (on the left panel) and the differential system of $\{C_S, C_R\}$ (on the right panel) with $s-$proliferation rate of sensitive cells, $r-$proliferation rate of resistant cells, $g-$transition rate from C_S to C_R

Figure 2 shows the diagrams of such population dynamics, and the system of ordinary differential equations that $\{C_S, C_R\}$ obey. The solution of the system (1) is

$$\begin{pmatrix} C_S(t) \\ C_R(t) \end{pmatrix} = \begin{pmatrix} e^{-(g-s)\,t} & 0 \\ \dfrac{g\,(e^{r\,t} - e^{-(g-s)\,t})}{g+r-s} & e^{r\,t} \end{pmatrix} \begin{pmatrix} C_S^0 \\ C_R^0 \end{pmatrix} \tag{2}$$

where $\{C_S(0), C_R(0)\} = \{C_S^0, C_R^0\}$. By (2), total population is

$$C_P(t) = \left(\frac{r-s}{g+r-s} C_S^0 \right) e^{-(g-s)\,t} + \left(\frac{g\,(C_S^0 + C_R^0) + (r-s)\,C_R^0}{g+r-s} \right) e^{r\,t}. \tag{3}$$

$C_P(t)$ is a positive function comprised of a linear combination of exponential growth ($e^{r\,t}$) and exponential decay ($e^{-(g-s)\,t}$) with positive coefficients. Despite the limitations of simple exponential growth models [24], we feel it is a reasonable place to start, since the relapse of tumor size starts when it is much smaller than its carrying capacity which results in almost exponential growth.

C_P has one and only one minimum point in $\{-\infty, \infty\}$, after which C_P increases monotonically. If $C_P'(0) = s\,C_S^0 + r\,C_R^0 \geq 0$, the drug is inefficient. ($C_P(t)$ is increasing on $t \geq 0$, see an example on Figure 3 (a)) Otherwise, if $C_P'(0) < 0$, the drug is effective in reducing tumor burden at the beginning, although it will eventually regrow (drug resistance; see an example on Figure 3 (b)).

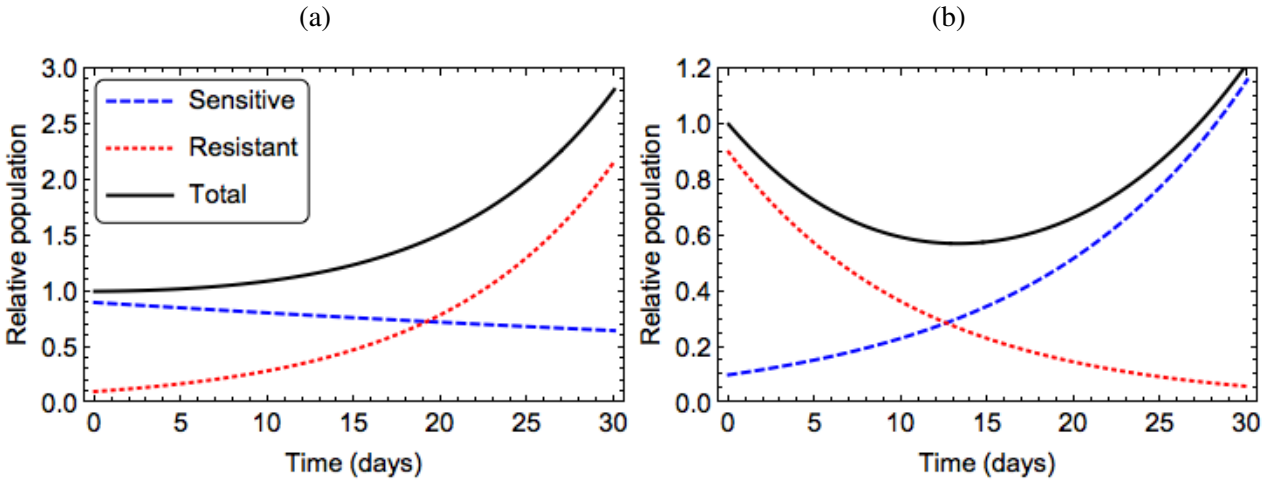

Figure 3: Representative population histories of sensitive and resistant cells and their summation with initial population makeup, $\{C_S^0, C_R^0\} = \{0.9, 0.1\}$. (a) increasing total population with $\{s, r, g\} = \{-0.01, 0.1, 0.001\}$; $C_P'(0) = 0.001 > 0$. (b) rebounding total population with $\{s, r, g\} = \{-0.09, 0.08, 0.001\}$; $C_P'(0) = -0.073 < 0$.

2.2 Cell population dynamics with a pair of collateral sensitivity drugs

Here, we describe the effect of a combined therapy with two drugs switched in turn, by extending the model for a single-drug administration (System (1)). Assuming that the drugs are collaterally sensitive to each other, cell population is classified into just two groups reacting to the two types of drugs in opposite ways. Depending on which drug to be administered, cells in the two groups will have different proliferation rates and direction of cell-type transition (see Figure 4). That is, the population dynamics of the two groups follow a piecewise continuous differential system consisting of a series of the system (1), each of which is assigned on a time slot bounded by times of

drug-switch.

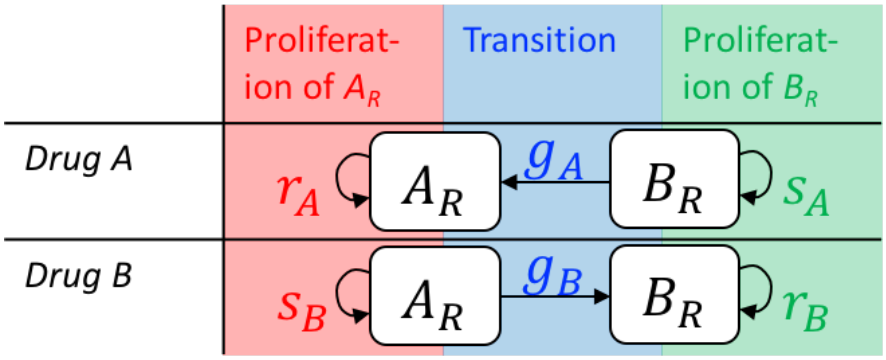

Figure 4: Population dynamics between A_R- population of cells resistant only to $DrugA$ and B_R- population of cells resistant only to $DrugB$ under the presence of $DrugA$, or $DrugB$. For each drug therapy, three drug-parameters of proliferations (colored red and green) and transition (colored blue) are involved.

In summary, we assume that

- there is a pair of collaterally sensitive drugs, $DrugA$ and $DrugB$, which are characterized by their own model parameters, $p_A = \{s_A, r_A, g_A\}$ and $p_B = \{s_B, r_B, g_B\}$ respectively,
- cell population can be split into two subpopulations, A_R - resistant to $DrugA$ and at the same time sensitive to $DrugB$, and B_R - resistant to $DrugB$ and sensitive to $DrugA$, and
- three types of factors determine the dynamical patterns, (i) drug parameters, $\{p_A,\ p_B\}$, (ii) initial population ratio $ApB_0 = A_R(0)/B_R(0)$ (assuming that $A_R(0) + B_R(0) = 1$), and (iii) drug switch schedule.

An example of histories of $\{A_R, B_R, A_R + B_R\}$ with a choice of the three factors is shown at Figure 5.

3 Analysis on therapy scheduling

3.1 Drug-switch timing

We explored possible strategies on choosing drug switch timing within our modeling setup. The first idea is relevant to clinical intuition: switching drug at the global minimum point of tumor size (T_{max}; see Figure 1 (a)), which is shown to exist uniquely in the previous section if and only if $C_R(0)/C_S(0) < -s/r$. The expression of T_{max} derived from our model is

$$T_{max}(\{s, r, g\}, RpS_0) = \frac{\ln\left[\dfrac{(g-s)(r-s)}{r(g(RpS_0+1)+RpS_0(r-s))}\right]}{g+r-s} \qquad \text{with } RpS_0 = \frac{C_R(0)}{C_S(0)}. \quad (4)$$

T_{max} depends on (i) the parameters of drug being administered, and (ii) initial population makeup. In the $DrugA$-based therapy, it is $T_{max}(p_A, ApB_0)$, and in the $DrugB$-based therapy, it is $T_{max}(p_B, 1/ApB_0)$.

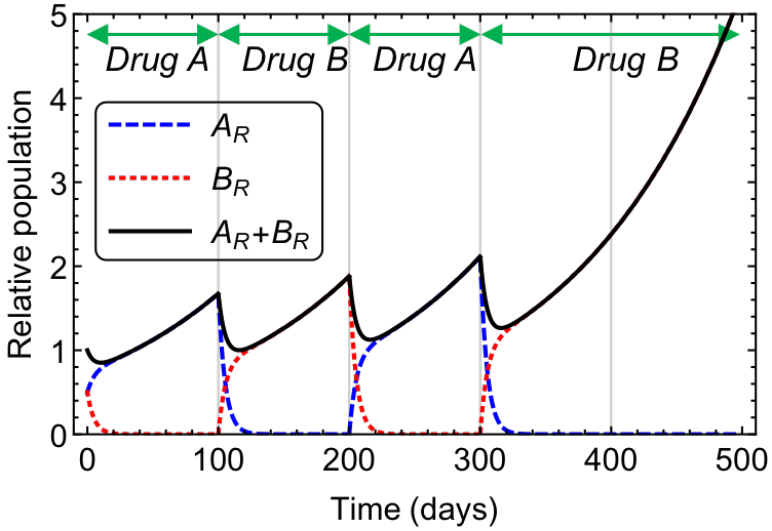

Figure 5: Representative plots describing dynamics of cell populations resistant to $DrugA$ (A_R), resistant to $DrugB$ (B_R) and total ($A_R + B_R$) during drug switches. Here, $p_A = p_B = \{-0.9, 0.08, 0.1\}/day$ and $\{A_R^0, B_R^0\} = \{0.5, 0.5\}$.

In addition to T_{max}, another time point with significant meaning is T_{min}, explained below. Since the decreasing rate is almost zero around T_{max} with no switch (see the black curve of Figure 5), we seek to find a way to expedite the decreasing rate by switching drug before T_{max}. To decide how much earlier to do so, we compared the derivative of $A_R + B_R$ under constant selective pressure (no switch) at an arbitrary time point, t_1, and compared it to the right derivative of $A_R + B_R$ with the drug-switch assigned at t_1. For example, if the first drug is $DrugA$ and the follow-up drug is $DrugB$, we compared

$$C'_P(t_1 \text{ given } \{s, r, g\} = p_A \text{ and } \{C_S^0, C_R^0\} = \{B_R(t_1), A_R(t_1)\}) \text{ from (3)},$$

and

$$C'_P(t_1 \text{ given } \{s, r, g\} = p_B \text{ and } \{C_S^0, C_R^0\} = \{A_R(t_1), B_R(t_1)\}) \text{ also from (3)}.$$

This comparison reveals that the two derivatives are equal at a specific point (this is T_{min}, see the yellow curve on Figure 6), the derivative of drug-switch is lower (higher in absolute value; higher decreasing rate) if $t_1 > T_{min}$ (see the blue and green curves on Figure 6), and the derivative of no-switch is lower if $t_1 < T_{min}$ (see the red curve on Figure 6).

T_{min} depends on the parameters for the first drug $\{s_1, r_1, g_1\}$ and for the second drug $\{s_2, r_2\}$, and initial population ratio between resistant cells and sensitive cells for the first drug RpS_0. Here, transition parameter of second drug (g_2), and respective values of the two populations are unnecessary in the evaluation of T_{min}, which is found to be

$$T_{min}(\{s_1, r_1, g_1\}, \{s_2, r_2\}, RpS_0) = \frac{\ln\left[\dfrac{(r_1 - s_1)(r_2 - s_1) + g_1(r_1 + r_2 - s_1 - s_2)}{(r_1 - s_2)(g_1 + RpS_0(g_1 + r_1 - s_1))}\right]}{g_1 + r_1 - s_1}. \quad (5)$$

In $DrugA$-to-$DrugB$ switch, it is $T_{min}(p_A, p_B, ApB_0)$, and in $DrugB$-to-$DrugA$ switch, it is $T_{min}(p_B, p_A, 1/ApB_0)$.

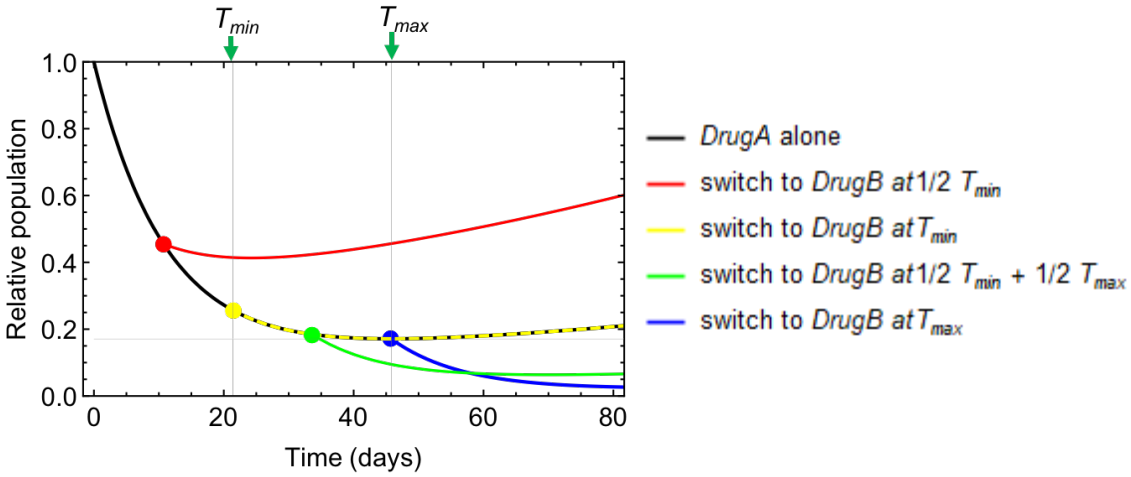

Figure 6: Comparison of total population curves with one-time drug-switch from $DrugA$ to $DrugB$ at different time points, (i) at $< T_{min}$ (worse than without-switch; red curve), (ii) at T_{min} (same as without-switch; yellow curve), (iii) between T_{min} and T_{max} (better than without-switch; green curve), and (iv) T_{max} (better than without-switch; blue curve). Each color of dot/curve represents cell population level on and after drug-switch of each switching strategy. The dashed curve mixed by yellow and black colors represent the yellow and black curves overlapped. Parameters: $p_A = p_B = \{-0.9, 0.08, 0.001\}/day$ and $\{A_R^0, B_R^0\} = \{0.1, 0.9\}$.

An important issue observed in Figure 6 is that the population curve with only one-time drug-switch after T_{min} (and before T_{max}, assuming that $T_{min} < T_{max}$) is not guaranteed to be lower than that of one-time switch at T_{max} over an entire time range. (i.e., the green curve relevant to the switch at $(T_{min} + T_{max})/2$ and the blue curve relevant to the switch at T_{max} intersect at $t \approx 58$ and the blue curve is lower after the time of the intersection). However, sequential drug switches started between T_{min} and T_{max} leave a possibility of finding a better drug schedule than the $T_{max}-$based strategy. Figure 7 shows possible choices of follow up switches (green and black curves) which achieve better results than $T_{max}-$switch (red curves), unlike the drug-switches started before T_{min} remaining less effective (magenta curve).

Optimal drug switch scheme will be discussed in detail in Section 4.2. The optimal scheduling for the example of Figure 5 starts with the first drug until T_{min} (blue curve for $0 < t \leq T_{min}$) followed by rapid exchange of the two drugs afterward (black curve for $t > T_{min}$). Switching before T_{max}, that is, before the drug has had its full effect, goes somewhat against clinical intuition, and is therefore an opportunity for unrealized clinical improvement based on a rationally scheduled switch at T_{min}. In order to realize this however, there are conditions about the order of T_{max} and T_{min} which must be satisfied. In particular:

$$\begin{cases} T_{min} < T_{max} \text{ if and only if } r_A r_B < s_A s_B \\ T_{min} = T_{max} \text{ if and only if } r_A r_B = s_A s_B \\ T_{min} > T_{max} \text{ if and only if } r_A r_B > s_A s_B. \end{cases} \tag{6}$$

In our analysis and simulations, we will deal with the cases mostly satisfying $r_A r_B < s_A s_B$, as otherwise we cannot expect improvement of clinical strategy using T_{min}, and more importantly as the choice of drugs not satisfying $r_A r_B < s_A s_B$ is not powerful to reduce cell population (explained in detail in the next section and Figure 8).

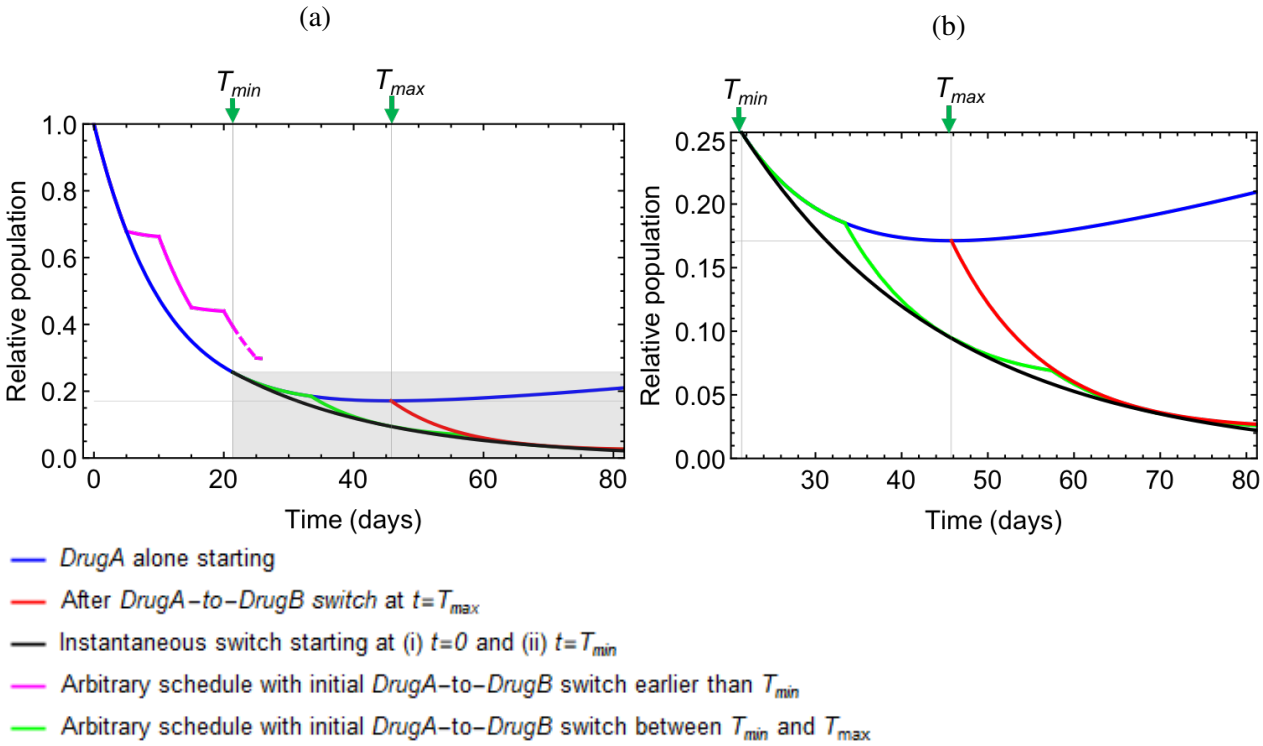

Figure 7: Total population curves with different therapy strategies with $p_A = p_B = \{-0.9, 0.08, 0.001\}/day$ and $\{A_R^0, B_R^0\} = \{0.1, 0.9\}$ (a) full range of relative population (b) enlargement of the shaded areas on (a)

The difference between T_{min} and T_{max} (T_{gap}), provides intuition on how much shorter the first drug administered than it is used to be.

$$\begin{aligned} T_{gap}(\{s_1, r_1, g_1\}, \{s_2, r_2\}) &:= T_{max}(\{s_1, r_1, g_1\}, RpS_0) - T_{min}(\{s_1, r_1, g_1\}, \{s_2, r_2\}, RpS_0) \\ &= \frac{\ln\left[\dfrac{(g_1 - s_1)(r_1 - s_1)(r_1 - s_2)}{r_1((r_1 - s_1)(r_2 - s_1) + g_1(r_1 + r_2 - s_1 - s_2))}\right]}{g_1 + r_1 - s_1} \end{aligned} \tag{7}$$

We studied sensitivity analysis on T_{gap} over a reasonable space of non-dimentionalized drug parameters in Appendix B. Expectedly, as the proliferation rates under the second drugs increases ($r_2 \uparrow$ and/or $s_2 \uparrow$), the optimal switching timing to the second drug is delayed ($T_{min} \uparrow$ and $T_{gap} \downarrow$). As r_1 increases, both T_{min} and T_{max} decrease. However, T_{max} decrease more than T_{min} does, so in overall T_{gap} decreases. s_1 and T_{gap} do not have a monotonic relationship. T_{gap} is increasing as s_1 is increasing in a range of relatively low values, but it turns into decreasing in relatively high values of s_1.

3.2 Population makeup and drug effect

In this section, we study how the degree of cellular heterogeneity and therapy effect are related, and checked the roles of T_{min} and T_{max} in the relationships. We defined a function of population makeup ApB based on the ratio between the two cell types,

$$ApB(t) := \frac{A_R(t)}{B_R(t)}.$$

Then, the ratio at T_{min} with $DrugA$-to-$DrugB$ switch (T^A_{min}) and with $DrugB$-to-$DrugA$ switch (T^B_{min}) are equivalent.

$$ApB(T^A_{min}) = ApB(T^B_{min}) = \frac{r_B - s_A}{r_A - s_B} := ApB^*. \tag{8}$$

At T_{max} with $DrugA$ (T^A_{max}), and with $DrugB$ (T^B_{max}), we have

$$ApB(T^A_{max}) = \frac{-s_A}{r_A},\ ApB(T^B_{max}) = \frac{r_B}{-s_B},$$

And, as $s < 0$ and $r > 0$, those values of ApB are all positive.

We next consider the level of drug effect at each ApB by taking the derivative of cell population under the presence of the drug. Fixing the total population, the derivative is defined by ApB in addition to the model parameters. We define this effect by

$$Ef(ApB) := \frac{d}{dt}(A_R(t) + B_R(t))\Big|^{p_A \text{ or } p_B}_{t=0, ApB_0 = ApB} \quad \text{with } A_R(0) + B_R(0) = 1.$$

The effects of $DrugA$ (specified by p_A) and $DrugB$ (specified by p_B) defined in this way are equivalent at ApB^*, by the definitions of T_{min} and ApB^*. The effect of $DrugA$ is larger if $ApB < ApB^*$, since the cell population resistant to $DrugA$ is relatively smaller than the population of the other cell type. Otherwise, $DrugB$ has a better effect. At the makeup of T^A_{max}, $DrugA$ has no effect on population reduction. If ApB is getting smaller than that, $DrugA$ becomes effective. And, the smaller ApB is, the better effect $DrugA$ has. Similarly the effect of Drug B is zero at $ApB(T^B_{max})$ and increases as ApB increases above $ApB(T^B_{max})$ (see Figure 8).

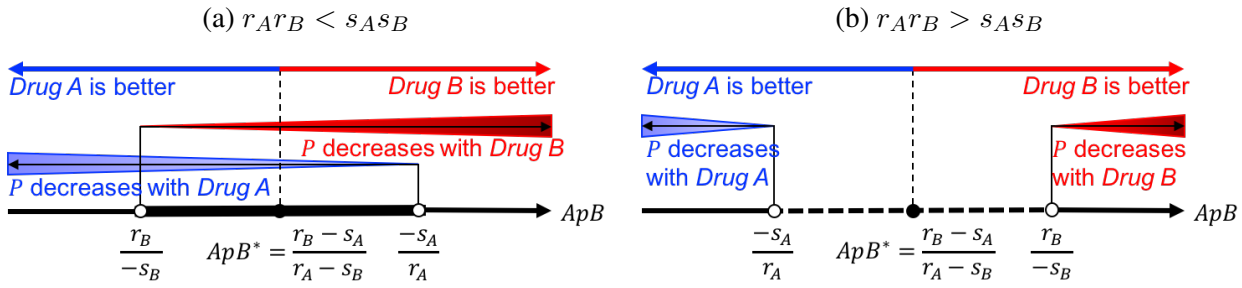

Figure 8: Effect of $DrugA$ and $DrugB$ over the axis of ApB. The two drugs have same effect at $ApB = ApB^*$, and have no effect at $ApB = -s_A/r_A$ (in case of $DrugA$) or $ApB = -r_B/s_B$ (in case of $DrugB$). The drug effect is getting bigger, as ApB is getting farther from the no-effect level to the direction of getting less cell population resistant to the drug.

The population makeup changes in the opposite direction. As $DrugA$ (or $DrugB$) therapy continues, ApB continues to increase (or decrease). So, if $DrugA$ (or $DrugB$) is given too long, it should go through a period of no or almost no effect around $ApB = -s_A/r_A$ (or around $ApB = -r_B/s_B$), but once the drug is switched after that, there will be a higher therapy effect with $DrugB$ (or with $DrugA$). Such two opposite aspect has shown to be balanced by switching drug when the population makeup reaches ApB^*.

Depending on the condition (6), the order of the three ratios at T_{min}, T^A_{min} and T^B_{max} changes. In particular, if $r_A r_B < s_A s_B$, there exists an interval of ApB, $(-r_B/s_B, -s_A/r_A)$, in which both drugs are effective in decreasing population, given the condition is satisfied. Otherwise, if $r_A r_B < s_A s_B$, no drug is effective when $ApB \in (-s_A/r_A, -r_B/s_B)$. These results are schematized in Figure 8.

3.3 Optimal scheduling and its clinical implementation

In this sections, we describe a drug-switch strategy to achieve the best effect possible with a pair of collaterally sensitive drugs. It is numerically found, and consists of two stages.

- **(Stage 1)** to reach to the population makeup with balanced drug effect (ApB^*), so the period lasts as long as T_{min} of the first drug
- **(Stage 2)** to give the two drugs with a proper ratio in period (represented by k or k'; see Figure 9) in order to keep ApB being constant at ApB^*, and switching them in a high frequency, represented by $\Delta t \approx 0$

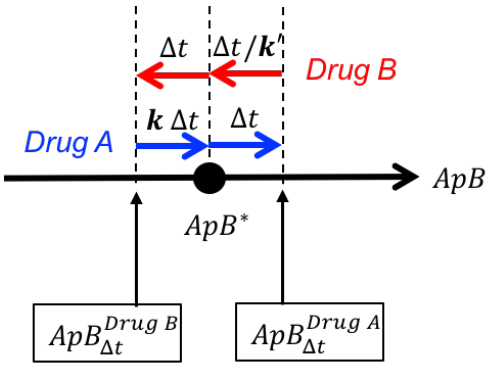

Figure 9: Diagram of the relationship between therapy duration (like Δt, $k\ \Delta t$, or $\Delta t/k'$) and change in ApB around ApB^*. Δt represents an arbitrary time interval (supposed to be small, $\Delta t \approx 0$), and k represents a specific quantity corresponding to such Δt and parameters of $DrugA$ and $DrugB$.

Both k and k' represents relative duration of $DrugA$ compared to duration of $DrugB$ in Stage 2. The explicit formulation of k can be derived from the solution of the differential equations (2) by (i) evaluating the level of ApB after Δt-long $DrugA$ therapy started with $ApB(0) = ApB^*$ ($ApB^{DrugA}_{\Delta t}$), and then, (ii) by measuring the time period taken to achieve ApB^* back from $ApB^{DrugA}_{\Delta t}$ through $DrugB$ therapy ($\Delta t'$), and finally (iii) taking ratio between the two therapy periods ($k = \Delta t/\Delta t'$). k depends on drug switch frequency and model parameters,

$$k = k(\Delta t, p_A, p_B). \tag{9}$$

Such k is consistent with k', which is the ratio similarly evaluated with $DrugB$ as first therapy and $DrugA$ as follow-up therapy, in the optimal case of instantaneous switching,

$$\begin{aligned}&\lim_{\Delta t\to 0} k(\Delta t, p_A, p_B) = \lim_{\Delta t\to 0} k'(\Delta t, p_A, p_B)\\ =&\frac{(r_A - s_B)((r_A - s_A)(r_B - s_A) + g_A(r_A + r_B - s_A - s_B))}{(r_B - s_A)((r_B - s_B)(r_A - s_B) + g_B(r_A + r_B - s_A - s_B))} := k^*(p_A, p_B).\end{aligned} \tag{10}$$

We studied how sensitive k^* (or $f^* = k^*/(1+k^*)$) is over a reasonable range of non-dimentionalized $\{p_A, p_B\}$ (see Appendix B for the detail). k^* (or f^*) increases, as r_A and/or s_B increases and as s_A and/or r_B increases.

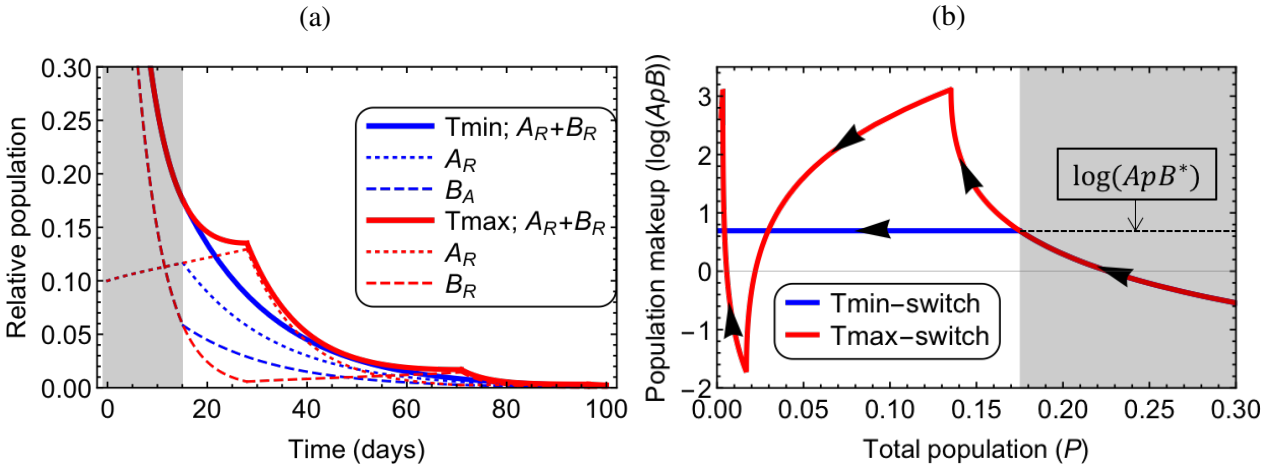

Figure 10: Comparison between dynamical trajectories of the optimal (T_{min} switch; blue curves) and a non-optimal (T_{max} switch; red curves) therapeutic strategies. Part of curves over Stage 1 and Stage 2 are drawn in gray and white backgrounds respectively. Parameters/conditions: $\{s_A, s_B\} = \{-0.18, -0.09\}$/day, $\{r_A, r_B\} = \{0.008, 0.016\}$/day, $\{g_A, g_B\} = \{0.00075, 0.00125\}$/day and $\{A_R^0, B_R^0\} = \{0.1, 0.9\}$

Figure 10 shows examples of population curves with the optimal strategy (T_{min} switch) and one non-optimal strategy (T_{max} switch) using the same choice of parameters/conditions. The visual comparison validates the better effect of the optimal strategy than the other strategy over a range of time (see Figure 10 (a)). Figure 10 (b) shows the typical pattern of ApB in the optimal therapy compared to the other, which is monotonically changing toward ApB^* in the first stage and staying still in the second stage.

For the sake of practicality of clinical application, instantaneous drug switch in Stage 2 could be approximated by high frequency switching with $\Delta t \gtrsim 0$ along with the corresponding $k(\Delta t)$ from (9), or k^* (10) independent from Δt. Expectedly, the smaller Δt is chosen, the closer to the ideal case with $\Delta t = 0$ (see Appendix C for the details).

Additionally, we have proved that the effect of instantaneous drug switch, with an arbitrary ratio in duration between two drugs (k), is consistent to the effect of mixed drug with relative dosage ratio which is also k (Theorem A.8 in Appendix). The theorem is used in the derivation of differential system/solution of optimal strategy (Theorem A.11 in Appendix). According to the results, in Stage 2 of optimal regimen, all types of populations, A_R, B_R and $A_R + B_R$, change with a same constant proliferation rate,

$$\lambda = \frac{r_A r_B - s_A s_B}{r_A + r_B - s_A - s_B}.$$

4 Stochastic studies on eradication time

In previous sections we utilized an entirely deterministic model of cancer. Cancers, however, are not deterministic, and without stochasticity in our system we could not model an important part

of cancer treatment: extinction. We therefore constructed a simple individual based model using a Gillespie algorithm to study this aspect of cross-sensitivity.

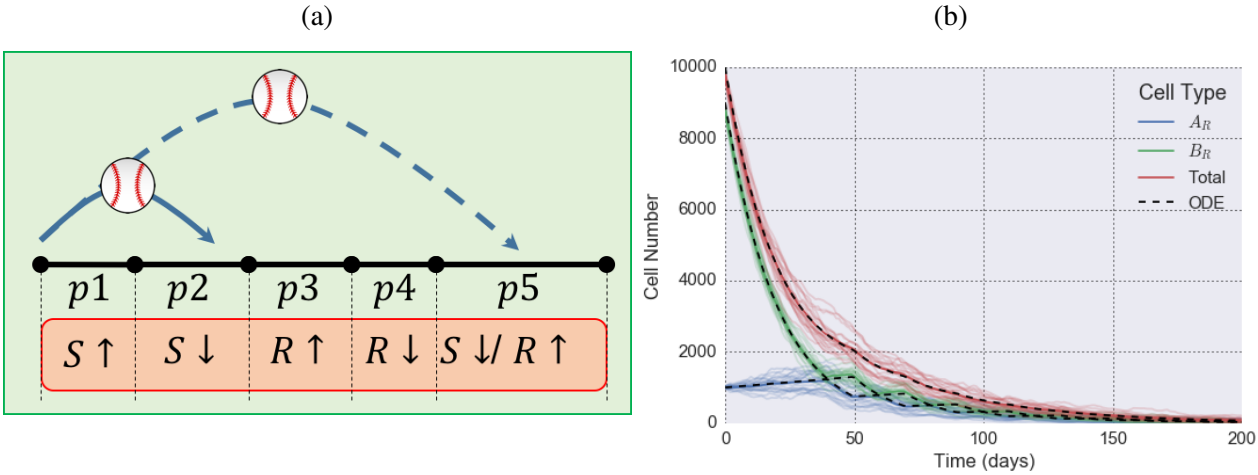

Figure 11: (a) Illustration of randomly possible events: birth or death in sensitive (S) or resistant (R) cell populations and transition from sensitive to resistant type. $\{p1, p2, p3, p4, p5\}$ represent the relative probabilities of the events occurring in the stochastic model. (b) Comparison between the stochastic process and the ODE model. The mean (thick curves) of multiple stochastic simulations (thin curves) are compared to the ODE solution (dashed curves). Parameters are $\{s_A, r_A, g_A | s_B, r_B, g_B | A_R^0, B_R^0\} = \{-0.05, 0.005, 0.0001 | -0.05, 0.005, 0.0001 | 1000, 9000\}$, birth rate + death rate (I_{stoch}) = 1.0.

Our stochastic model depends not only on net proliferation rates (s, r, see Equation (1)) but also on the combination of birth rates (b_S, b_R) and death rates (d_S, d_R) where $s = b_S - d_S$ and $r = b_R - d_R$. These five parameters (b_s, b_r, d_s, d_r, g) govern the probabilities of events occurring (Figure 11 (a)). The time at which one of these events occurs is determined by an exponential probability distribution, and we represent the algorithm as pseudo-code thus:

(Step 1) Initialize $\{S(0), R(0)\} = \{C_S^0, C_R^0\}$.

(Step 2) Update from t to $t + dt$:

(random number generation)
$rt \sim U[0, 1]$, $re \sim U[0, 1]$
$a = (b_S + d_S + g)S(t) + (b_R + d_R)R(t)$
$dt = -\log(rt)/a$
$\{p1, p2, p3, p4, p5\} = \{b_S S(t), d_S S(t), b_R R(t), d_R R(t), g\ S(t)\}/a$

if $re < p1$, then $S(t + dt) = S(t) + 1$
else if $re < p2 + p1$, then $S(t + dt) = S(t) - 1$
else if $re < p3 + p2 + p1$, then $R(t + dt) = R(t) + 1$
else if $re < p4 + p3 + p2 + p1$, then $R(t + dt) = R(t) - 1$
else, $S(t + dt) = S(t) - 1$ and $R(t + dt) = R(t) + 1$

(Step 3) $t \leftarrow t + dt$ and repeat **(Step 2)** until a set time has passed or extinction has occurred.

We expanded the stochastic process for a single drug to treatment with two drugs being switched in turn, as in our ODE system. (See Appendix D, for the details of the computational code.) Figure 11 (b) shows the consistency between the mean behavior of the stochastic model and the ODE system.

Despite the generally similar patterns of population curves simulated with same $\{s, r, g\}$-type of parameters and initial conditions, they are significantly different in terms of elimination time if birth/death combinations are different. So, we studied elimination times simulated with different combinations of birth/death rates, with a choice of fixed proliferation rates (as well as other fixed transition rates and initial condition). We defined an index to represent different levels of birth and death rate combinations:

$$I_{stoch} = b_{I,J} + d_{I,J} \qquad \text{for } I \in \{S, R\} \text{ and } J \in \{A, B\}$$

where I indicates a type of sensitivity or resistance and J does a type of drug. Given a specific net proliferation rate ($b_{I,J} - d_{I,J}$), the larger the index is, the larger both birth ($b_{I,J}$) and death ($d_{I,J}$) rates are.

(a) Low I_{stoch} (b) High I_{stoch}

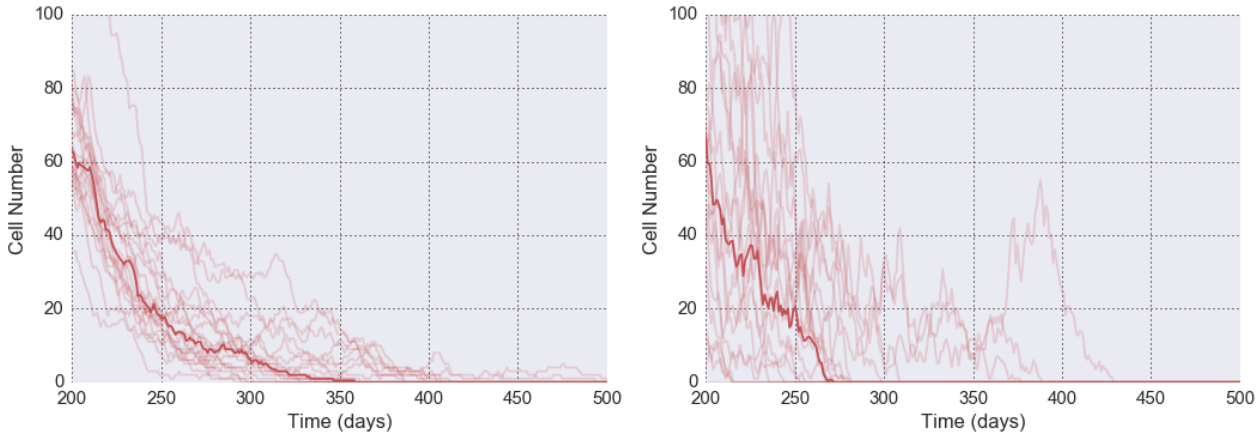

Figure 12: Comparison between stochastic simulations with different levels of birth/death combinations: $I_{stoch} = 0.1$ (a) and $I_{stoch} = 1.0$ (b). For each case, 20 simulated cell number histories are shown in thin curves with their median in a thick curve. Same values are used for other parameters/conditions, in both cases: $\{s_A, r_A, g_A | s_B, r_B, g_B | A_R^0, B_R^0\} = \{-0.05, 0.005, 0.0001 | -0.05, 0.005, 0.0001 | 1000, 9000\}$.

Increased I_{stoch} result in larger fluctuations (Figure 12 (b)), these fluctuations then increase the probability of reaching an absorbing state, in this case extinction. The relationship between I_{stoch} and extinction time is shown in Figure 13. The relationship is significant ($p < 0.05$ and $r^2 = 0.1726$ with slope= -93.68 days^2).

5 Conclusions and discussion

The emergence of resistance to our presently best therapies is a sad, and conserved reality in the oncology clinics today. While much effort has been put into novel drug discovery to combat this, there is also a growing interest in determining optimal sequences, or cycles of drugs that induce

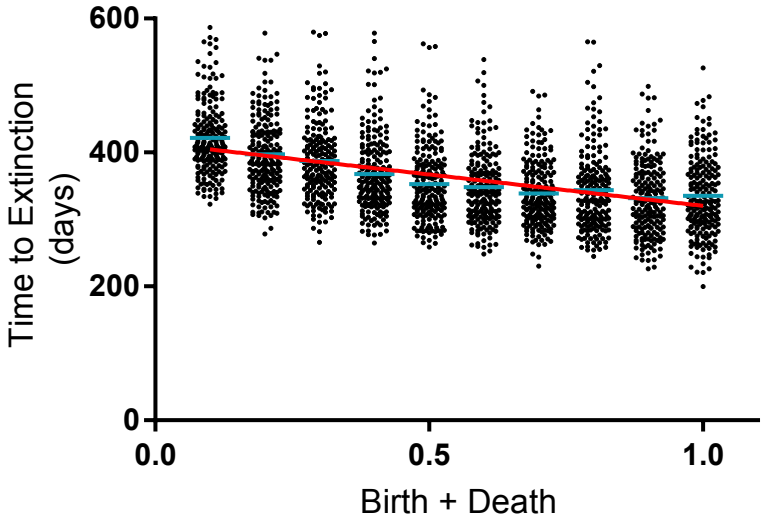

Figure 13: Relationship between birth-death combinations (I_{stoch}; 0.1 to 1.0 with intervals of 0.1) and simulated extinction time in 200 replicates. Parameters are $\{s_A, r_A, g_A | s_B, r_B, g_B | A_R^0, B_R^0\} = \{-0.05, 0.005, 0.0001 | -0.05, 0.005, 0.0001 | 1000, 9000\}$. Regression (red line) is $y = -93.68x + 414$ (slope has p<0.05 and $r^2 = 0.1726$).Cyan lines show mean values.

continued (or collateral) sensitivity. To study this second scenario, we proposed a simple dynamical systems model of tumor evolution in a heterogeneous tumor composed of two cell phenotypes. While in reality, cell phenotype can be defined in many ways, here we completely describe it by considering only sensitivity (or resistance) to a pair of collaterally sensitive drugs, which is encoded in their differential growth rates in specific conditions. While the resulting mathematical model conveys only simple, but essential, features of cell population dynamics, it does yield analytical solutions that more complex models can not.

Our original motivation was to consider more complicated sequences, or cycles of drug therapy, however, the model presented herein is difficult to apply for an expanded system of more than two drugs. On the other hand, the cell classification used by other [11, 12, 21, 22, 25] considers sensitivity and resistance independently, or even specifically to a given, abstracted, genotype [26, 27]. Therefore, in case of 2 drugs, there are $2^2 = 4$ groups, (i) sensitive to both drugs, (ii) and (iii) resistant to only one drug, and (iv) resistant to both drugs. This formulation could be expanded and applied to more than two drugs [11, 25], and we will consider it in future work.

The simplicity of our exponential growth/decay model is owing to the assumption of a constant growth rate. Use of exponential growth is likely not overly inappropriate, as we are most interested in the development of resistance – and resistance is typically thought to begin when tumor burden is much smaller than carrying capacity. However, the assumption might have oversimplified patterns of cell growth, which is assumed to be non-exponential by others (e.g. logistic growth [24, 28, 29]), due to the limited space and resource of human body for tumor growth, as well as increasing levels of resistance (increasing growth rates) in the face of continued selective pressure [30]. We will consider the concept of changing growth rate in terms of time and population density, and explore its effect on our analytical results (like T_{gap}, ApB^*, k^* and etc.) in future work.

We provided a strategy of drug-switch which can yield the theoretically best possible effect in

decreasing cell populations. The strategy is defined explicitly in terms of these parameters relevant to the used drugs, so the usefulness of our analytic results are challenged by the availability of drug parameters. Drug parameters for several drugs are known based on *in vitro* experiment or clinical studies [31, 32]. However, it is not available for all drugs, and even the results measured *in vitro* would likely change from one patient to the next. Because of this, we propose focusing our future work on learning to parameterize models of this type from individual patient response data. Examples of parameterizing patient response from imaging [33] as well as blood based markers [34] already exist, suggesting this is a reasonable goal in the near term.

In our optimized treatment regimen we must first apply $DrugA$ (if $DrugA$ is better at the initial time, i.e., $ApB(0) < ApB^*$; see Figure 8). Surprisingly the ideal treatment course switches to $DrugB$ while $DrugA$ is still effective at reducing total population. Since treatment should ideally switch before the tumor relapses our study justifies the search for techniques that either identify or predict resistance mechanisms early. Our study also argues against the opposite extreme, wherein resistant cells are targeted at the beginning of treatment. The preponderance of cells sensitive to the standard of care makes this treatment initially ideal, and does not preclude eventual success in our model. Further, the rapid tumor size reduction associated with targeting the larger, sensitive, population first could be clinically meaningful.

Our stochastic model allowed us to explore the contributions of cell birth and death separately, as opposed to the ODE which could only consider the net growth rate. These parameters can be altered in cancer since cancer treatments have various cytostatic and cytotoxic effects, and therefore different treatments can have different effects on death and birth. In our model, increasing the total birth and death rate (as opposed to the net growth rate) caused extinction earlier in time (Figure 12, Figure 13). This can be explained by the fact that extinction is the only absorbing state in our model, and therefore higher death rates determine when extinction occurs, even when birth rates are also higher. Our stochastic model therefore suggests that highly cytotoxic drugs (even those with correspondingly minimal cytostatic effects) are more effective at eliminating tumors, at least when the tumor population is small.

Other possible ideas of future work involve comparison between different models. A recent area of debate concerns whether cycling, or directly mixing therapies is superior. In our simplified model, we show under certain regimes of (timing of) drug switching, the effect of drug cycling and drug mixing strategies are equivalent (Theorem A.8). Further exploring the ramifications of this through modeling of timing and combinations would be of value [35, 36].

In summary, we have presented a simple model of a heterogeneous two phenotype tumour with evolution between resistant and sensitive states. We derive exact analytic solutions for tumor response in temporally changing drug conditions and find an optimal regimen which involves drug switching after a specific, critical time point, which critically, occurs before resistance would normally be clinically evident. While our model is highly simplified, we have identified several opportunities to improve our understanding and treatment of drug resistance, and also future opportunities for new modelling endeavors.

References

[1] C. Holohan, S. Van Schaeybroeck, D. B. Longley, and P. G. Johnston, "Cancer drug resistance: an evolving paradigm," *Nature reviews. Cancer*, vol. 13, no. 10, p. 714, 2013.

[2] R. J. Gillies, D. Verduzco, and R. A. Gatenby, "Evolutionary dynamics unifies carcinogenesis and cancer therapy," *Nature reviews. Cancer*, vol. 12, no. 7, p. 487, 2012.

[3] N. Amirouchene-Angelozzi, C. Swanton, and A. Bardelli, "Tumor evolution as a therapeutic target," *Cancer Discovery*, vol. 7, no. 8, pp. 805–817, 2017.

[4] M.-T. Dimanche-Boitrel, C. Garrido, and B. Chauffert, "Kinetic resistance to anticancer agents," *Cytotechnology*, vol. 12, no. 1-3, pp. 347–356, 1993.

[5] A. Thomas, S. El Rouby, J. C. Reed, S. Krajewski, R. Silber, M. Potmesil, and E. W. Newcomb, "Drug-induced apoptosis in b-cell chronic lymphocytic leukemia: relationship between p53 gene mutation and bcl-2/bax proteins in drug resistance.," *Oncogene*, vol. 12, no. 5, pp. 1055–1062, 1996.

[6] C. Scheel and R. A. Weinberg, "Phenotypic plasticity and epithelial-mesenchymal transitions in cancer and normal stem cells?," *International journal of cancer*, vol. 129, no. 10, pp. 2310–2314, 2011.

[7] D. J. Hutchison, "Cross resistance and collateral sensitivity studies in cancer chemotherapy," *Advances in cancer research*, vol. 7, pp. 235–350, 1963.

[8] A. Dhawan, D. Nichol, F. Kinose, M. E. Abazeed, A. Marusyk, E. B. Haura, and J. G. Scott, "Collateral sensitivity networks reveal evolutionary instability and novel treatment strategies in alk mutated non-small cell lung cancer," *Scientific Reports*, vol. 7, 2017.

[9] L. Imamovic and M. O. Sommer, "Use of collateral sensitivity networks to design drug cycling protocols that avoid resistance development," *Science translational medicine*, vol. 5, no. 204, pp. 204ra132–204ra132, 2013.

[10] D. Nichol, J. Rutter, C. Bryant, P. Jeavons, A. Anderson, R. Bonomo, and J. Scott, "Collateral sensitivity is contingent on the repeatability of evolution," *bioRxiv*, p. 185892, 2017.

[11] C. Tomasetti and D. Levy, "An elementary approach to modeling drug resistance in cancer," *Mathematical biosciences and engineering: MBE*, vol. 7, no. 4, p. 905, 2010.

[12] J. Goldie and A. Coldman, "Quantitative model for multiple levels of drug resistance in clinical tumors.," *Cancer treatment reports*, vol. 67, no. 10, pp. 923–931, 1983.

[13] N. L. Komarova and D. Wodarz, "Evolutionary dynamics of mutator phenotypes in cancer," *Cancer Research*, vol. 63, no. 20, pp. 6635–6642, 2003.

[14] J. Goldie, "Rationale for the use of alternating non-cross-resistant chemotherapy," *Cancer Treat Rep*, vol. 66, pp. 439–449, 1982.

[15] E. Gaffney, "The application of mathematical modelling to aspects of adjuvant chemotherapy scheduling," *Journal of mathematical biology*, vol. 48, no. 4, pp. 375–422, 2004.

[16] E. Gaffney, "The mathematical modelling of adjuvant chemotherapy scheduling: incorporating the effects of protocol rest phases and pharmacokinetics," *Bulletin of mathematical biology*, vol. 67, no. 3, pp. 563–611, 2005.

[17] E. A. Boston and E. A. Gaffney, "The influence of toxicity constraints in models of chemotherapeutic protocol escalation," *Mathematical medicine and biology: a journal of the IMA*, vol. 28, no. 4, pp. 357–384, 2011.

[18] J. G. Scott, A. G. Fletcher, A. R. Anderson, and P. K. Maini, "Spatial metrics of tumour vascular organisation predict radiation efficacy in a computational model," *PLoS computational biology*, vol. 12, no. 1, p. e1004712, 2016.

[19] K. A. Rejniak, "A single-cell approach in modeling the dynamics of tumor microregions," *Math. Biosci. Eng*, vol. 2, no. 3, pp. 643–655, 2005.

[20] J.-H. Chen, Y.-H. Kuo, and H. P. Luh, "Optimal policies of non-cross-resistant chemotherapy on goldie and coldmans cancer model," *Mathematical biosciences*, vol. 245, no. 2, pp. 282–298, 2013.

[21] A. A. Katouli and N. L. Komarova, "The worst drug rule revisited: mathematical modeling of cyclic cancer treatments," *Bulletin of mathematical biology*, vol. 73, no. 3, pp. 549–584, 2011.

[22] J. Goldie and A. Coldman, "A mathematic model for relating the drug sensitivity of tumors to their spontaneous mutation rate.," *Cancer treatment reports*, vol. 63, no. 11-12, pp. 1727–1733, 1979.

[23] A. Coldman and J. Goldie, "A model for the resistance of tumor cells to cancer chemotherapeutic agents," *Mathematical Biosciences*, vol. 65, no. 2, pp. 291–307, 1983.

[24] P. Gerlee, "The model muddle: in search of tumor growth laws," *Cancer research*, vol. 73, no. 8, pp. 2407–2411, 2013.

[25] J. H. Goldie and A. J. Coldman, *Drug resistance in cancer: mechanisms and models*. Cambridge University Press, 2009.

[26] N. L. Komarova and D. Wodarz, "Drug resistance in cancer: principles of emergence and prevention," *Proceedings of the National Academy of Sciences of the United States of America*, vol. 102, no. 27, pp. 9714–9719, 2005.

[27] D. Nichol, P. Jeavons, A. G. Fletcher, R. A. Bonomo, P. K. Maini, J. L. Paul, R. A. Gatenby, A. R. Anderson, and J. G. Scott, "Steering evolution with sequential therapy to prevent the emergence of bacterial antibiotic resistance," *PLoS computational biology*, vol. 11, no. 9, p. e1004493, 2015.

[28] S. J. Berry, D. S. Coffey, P. C. Walsh, and L. L. Ewing, "The development of human benign prostatic hyperplasia with age," *The Journal of urology*, vol. 132, no. 3, pp. 474–479, 1984.

[29] N. C. Atuegwu, L. R. Arlinghaus, X. Li, A. B. Chakravarthy, V. G. Abramson, M. E. Sanders, and T. E. Yankeelov, "Parameterizing the logistic model of tumor growth by dw-mri and dce-mri data to predict treatment response and changes in breast cancer cellularity during neoadjuvant chemotherapy," *Translational oncology*, vol. 6, no. 3, pp. 256–264, 2013.

[30] J. Scott and A. Marusyk, "Somatic clonal evolution: A selection-centric perspective," *Biochimica et Biophysica Acta (BBA)-Reviews on Cancer*, vol. 1867, no. 2, pp. 139–150, 2017.

[31] T. L. Jackson and H. M. Byrne, "A mathematical model to study the effects of drug resistance and vasculature on the response of solid tumors to chemotherapy," *Mathematical biosciences*, vol. 164, no. 1, pp. 17–38, 2000.

[32] W. H. Wilson, J. Teruya-Feldstein, T. Fest, C. Harris, S. M. Steinberg, E. S. Jaffe, and M. Raffeld, "Relationship of p53, bcl-2, and tumor proliferation to clinical drug resistance in non-hodgkin9s lymphomas," *Blood*, vol. 89, no. 2, pp. 601–609, 1997.

[33] K. R. Swanson, R. C. Rockne, J. Claridge, M. A. Chaplain, E. C. Alvord, and A. R. Anderson, "Quantifying the role of angiogenesis in malignant progression of gliomas: in silico modeling integrates imaging and histology," *Cancer research*, vol. 71, no. 24, pp. 7366–7375, 2011.

[34] B. Werner, J. G. Scott, A. Sottoriva, A. R. Anderson, A. Traulsen, and P. M. Altrock, "The cancer stem cell fraction in hierarchically organized tumors can be estimated using mathematical modeling and patient-specific treatment trajectories," *Cancer research*, vol. 76, no. 7, pp. 1705–1713, 2016.

[35] R. E. Beardmore, R. Peña-Miller, F. Gori, and J. Iredell, "Antibiotic cycling and antibiotic mixing: which one best mitigates antibiotic resistance?," *Molecular biology and evolution*, vol. 34, no. 4, pp. 802–817, 2017.

[36] R. Pena-Miller and R. Beardmore, "Antibiotic cycling versus mixing: the difficulty of using mathematical models to definitively quantify their relative merits.," 2010.

Appendix A Derivations of explicit expressions

Definition $\mathbb{D}_A := \begin{pmatrix} r_A & g_A \\ 0 & s_A - g_A \end{pmatrix}, \mathbb{D}_B := \begin{pmatrix} s_B - g_B & 0 \\ g_B & r_B \end{pmatrix}, V(t) := \begin{pmatrix} A_R(t) \\ B_R(t) \end{pmatrix},$

$$\mathbb{M}_A(t) := \begin{pmatrix} e^{r_A\, t} & \dfrac{g_A\,(e^{r_A\, t} - e^{-(g_A - s_A)\, t})}{g_A + r_A - s_A} \\ 0 & e^{-(g_A - s_A)\, t} \end{pmatrix}, \mathbb{M}_B(t) := \begin{pmatrix} e^{-(g_B - s_B)\, t} & 0 \\ \dfrac{g_B\,(e^{r_B\, t} - e^{-(g_B - s_B)\, t})}{g_B + r_B - s_B} & e^{r_B\, t} \end{pmatrix},$$

$\mathbb{A}_\epsilon := \mathbb{M}_A(f\,\epsilon), \mathbb{B}_\epsilon := \mathbb{M}_B((1-f)\epsilon),$

$$\min\left[V(t_1), V(t_2), \cdots, V(t_n)\right] := \begin{pmatrix} \min\left[A_R(t_1), A_R(t_2), \cdots, A_R(t_n)\right] \\ \min\left[A_R(t_1), A_R(t_2), \cdots, A_R(t_n)\right] \end{pmatrix},$$

$$\max\left[V(t_1), V(t_2), \cdots, V(t_n)\right] := \begin{pmatrix} \max\left[A_R(t_1), A_R(t_2), \cdots, A_R(t_n)\right] \\ \max\left[A_R(t_1), A_R(t_2), \cdots, A_R(t_n)\right] \end{pmatrix}.$$

Proposition A.1. *Under the therapy with Drug A,*

$$V'(t) = \mathbb{D}_A\, V(t),\ V(t_0 + \Delta t) = \mathbb{M}_A(\Delta t)\, V(t_0).$$

Under the therapy with Drug B,

$$V'(t) = \mathbb{D}_B\, V(t),\ V(t_0 + \Delta t) = \mathbb{M}_B(\Delta t)\, V(t_0).$$

A.1 Differential system of instantaneous drug switch

Proposition A.2. *Both A_R and B_R are monotonic functions under either therapy. Under the presence of Drug A, A_R is increasing, and B_R is decreasing. And, under the presence of Drug B, A_R is decreasing, and B_R is increasing.*

Proposition A.3. $\mathbb{A}_\epsilon|_{\epsilon=0} = \mathbb{B}_\epsilon|_{\epsilon=0} = I_2$ *for all* $0 \le f \le 1$

Proposition A.4. $\left.\frac{d}{d\epsilon}\mathbb{A}_\epsilon\right|_{\epsilon=0} = f\ \mathbb{D}_A,\ \left.\frac{d}{d\epsilon}\mathbb{B}_\epsilon\right|_{\epsilon=0} = (1-f)\mathbb{D}_B$ *for all* $0 \le f \le 1$

Lemma A.5. $\lim_{\epsilon\to 0}\frac{\mathbb{B}_\epsilon\mathbb{A}_\epsilon - I_2}{\epsilon} = f\ \mathbb{D}_A + (1-f)\mathbb{D}_B$ *for all* $0 \le f \le 1$

Proof.

$$\begin{aligned}\lim_{\epsilon\to 0}\frac{\mathbb{B}_\epsilon\mathbb{A}_\epsilon - I_2}{\epsilon} &= \lim_{\epsilon\to 0}\frac{\frac{d}{d\epsilon}(\mathbb{B}_\epsilon\mathbb{A}_\epsilon - I_2)}{\frac{d}{d\epsilon}\epsilon} && \text{(by L'Hospital's Rule)}\\ &= \lim_{\epsilon\to 0}\frac{\frac{d\mathbb{B}_\epsilon}{d\epsilon}\mathbb{A}_\epsilon + \mathbb{B}_\epsilon\frac{d\mathbb{A}_\epsilon}{d\epsilon}}{1}\\ &= f\ \mathbb{D}_A + (1-f)\mathbb{D}_B && \text{(by Propositions A.3 - A.4)}\end{aligned}$$

□

Lemma A.6. $\lim_{\epsilon\to 0}\frac{(\mathbb{B}_\epsilon\mathbb{A}_\epsilon)^n - I_2}{n\,\epsilon} = f\ \mathbb{D}_A + (1-f)\mathbb{D}_B$ *for any positive integer,* n*, and for all* $0 \le f \le 1$

Proof. Let $F(n) \coloneqq \lim_{\epsilon\to 0}\frac{(\mathbb{B}_\epsilon\mathbb{A}_\epsilon)^n - I_2}{n\,\epsilon}$ and $L \coloneqq f\ \mathbb{D}_A + (1-f)\mathbb{D}_B$.
Then, we need to prove that $F(n) = L$ for $n = 1, 2, 3, ...$
If $n = 1$,

$$F(n) = F(1) = L \qquad \text{(by Lemma A.5)}$$

Otherwise, if $n \ge 2$ and $F(m) = L$ for all $1 \le m \le n-1$,

$$\begin{aligned}F(n) &= \lim_{\epsilon\to 0}\frac{(\mathbb{B}_\epsilon\mathbb{A}_\epsilon)^n - I_2}{n\,\epsilon}\\ &= \lim_{\epsilon\to 0}\frac{((\mathbb{B}_\epsilon\mathbb{A}_\epsilon)^{n-1} - I_2)(\mathbb{B}_\epsilon\mathbb{A}_\epsilon) + (\mathbb{B}_\epsilon\mathbb{A}_\epsilon - I_2)}{n\,\epsilon}\\ &= \frac{n-1}{n}\lim_{\epsilon\to 0}\frac{((\mathbb{B}_\epsilon\mathbb{A}_\epsilon)^{n-1} - I_2)(\mathbb{B}_\epsilon\mathbb{A}_\epsilon)}{(n-1)\,\epsilon} + \frac{1}{n}\lim_{\epsilon\to 0}\frac{\mathbb{B}_\epsilon\mathbb{A}_\epsilon - I_2}{\epsilon}\\ &= \frac{n-1}{n}F(n-1) + \frac{1}{n}F(1)\\ &= \frac{n-1}{n}L + \frac{1}{n}L && \text{(by the inductive assumption)}\\ &= L\end{aligned}$$

Therefore, proved. □

Lemma A.7. $\lim_{\epsilon\to 0}\frac{\mathbb{A}_\epsilon(\mathbb{B}_\epsilon\mathbb{A}_\epsilon)^n - I_2}{(n+f)\,\epsilon} = \frac{(n+1)f}{n+f}\,\mathbb{D}_A + \frac{n(1-f)}{n+f}\mathbb{D}_B$ *for any positive integer,* n*, and for all* $0 \le f \le 1$

Proof. Using mathematical induction, if n=1,

$$
\begin{aligned}
&\lim_{\epsilon\to 0}\frac{\mathbb{A}_\epsilon(\mathbb{B}_\epsilon\mathbb{A}_\epsilon)-I_2}{(1+f)\,\epsilon}\\
=&\frac{1}{1+f}\lim_{\epsilon\to 0}\frac{\mathbb{A}_\epsilon(\mathbb{B}_\epsilon\mathbb{A}_\epsilon-I_2)+(\mathbb{A}_\epsilon-I_2)}{\epsilon}\\
=&\frac{1}{1+f}\left[\lim_{\epsilon\to 0}\mathbb{A}_\epsilon\lim_{\epsilon\to 0}\frac{\mathbb{B}_\epsilon\mathbb{A}_\epsilon-I_2}{\epsilon}+\lim_{\epsilon\to 0}\frac{\mathbb{A}_\epsilon-I_2}{\epsilon}\right]\\
=&\frac{1}{1+f}\left[I_2(f\,\mathbb{D}_A+(1-f)\mathbb{D}_B)+\frac{d}{d\epsilon}\mathbb{A}_\epsilon\Big|_{\epsilon=0}\right] \qquad \text{(by Proposition A.3 and Lemma A.5)}\\
=&\frac{1}{1+f}\left[(f\,\mathbb{D}_A+(1-f)\mathbb{D}_B)+k\,\mathbb{D}_A\right] \qquad \text{(by Proposition A.4)}\\
=&\frac{2\,f}{1+f}\mathbb{D}_A+\frac{1-f}{1+f}\mathbb{D}_B \qquad \text{The equality is true for } n=1
\end{aligned}
$$

If $n\geq 2$, and the equality works for all integers $1\leq m\leq n-1$,

$$
\begin{aligned}
&\lim_{\epsilon\to 0}\frac{\mathbb{A}_\epsilon(\mathbb{B}_\epsilon\mathbb{A}_\epsilon)^n-I_2}{(n+f)\,\epsilon}\\
=&\frac{1}{n+f}\left[\lim_{\epsilon\to 0}\frac{(\mathbb{A}_\epsilon(\mathbb{B}_\epsilon\mathbb{A}_\epsilon)^{n-1}-I_2)(\mathbb{B}_\epsilon\mathbb{A}_\epsilon)+(\mathbb{B}_\epsilon\mathbb{A}_\epsilon-I_2)}{\epsilon}\right]\\
=&\frac{1}{n+f}\left[((n-1)+f)\lim_{\epsilon\to 0}\frac{(\mathbb{A}_\epsilon(\mathbb{B}_\epsilon\mathbb{A}_\epsilon)^{n-1}-I_2)}{((n-1)+f)\epsilon}\lim_{\epsilon\to 0}(\mathbb{B}_\epsilon\mathbb{A}_\epsilon)+\lim_{\epsilon\to 0}\frac{\mathbb{B}_\epsilon\mathbb{A}_\epsilon-I_2}{\epsilon}\right]\\
=&\frac{1}{n+f}\left[((n-1)+f)\left(\frac{n\,f}{(n-1)+f}\,\mathbb{D}_A+\frac{(n-1)(1-f)}{(n-1)+f}\mathbb{D}_B\right)(I_2\;I_2)\right.\\
&\left.+(f\,\mathbb{D}_A+(1-f)\mathbb{D}_B)\right]\\
&\qquad\text{(by the inductive assumption and Proposition A.3 and Lemma A.5)}\\
=&\frac{(n+1)f}{n+f}\,\mathbb{D}_A+\frac{n(1-f)}{n+f}\mathbb{D}_B \qquad \text{(The equality is true for } n\geq 2)
\end{aligned}
$$

Therefore, proved. □

Theorem A.8. *If Drug A and Drug B are prescribed in turn with relative intensity f and $1-f$, and are switched instantaneously, V obeys*

$$\frac{dV}{dt}=(f\,\mathbb{D}_A+(1-f)\mathbb{D}_B)V$$

Proof. For any time point t_0, let us define $V_\epsilon(t)$ as a vector-valued function of $A_R(t)$ and $B_R(t)$ describing cell population dynamics under periodic therapy started on t_0 with $DrugA$ assigned on $t_0+m\,\epsilon\leq t<t_0+(m+f)\epsilon$ and $DrugB$ on $t_0+(m+f)\epsilon\leq t<t_0+(m+1)\epsilon$ for $m=0,1,2,3,\ldots$. Then, by Proposition A.1 and the definitions of $\mathbb{A}$ and $\mathbb{B}$,

$$V_\epsilon(t_0+m\,\epsilon)=(\mathbb{B}_\epsilon\mathbb{A}_\epsilon)^m\,V(t_0),\qquad V_\epsilon(t_0+(m+f)\epsilon)=\mathbb{A}_\epsilon(\mathbb{B}_\epsilon\mathbb{A}_\epsilon)^m\,V(t_0)\qquad\cdots(*1)$$

where $V(t_0)=\begin{pmatrix}A_R(t_0)\\B_R(t_0)\end{pmatrix}$. And, $V_0(t)$ represents instantaneous drug switch.

For any $\Delta t>0$ and any positive integer n, there exists $\epsilon=\epsilon(n,\Delta t)$ such that

$$\frac{\Delta t}{n+1}<\epsilon\leq\frac{\Delta t}{n}\qquad\text{or}\qquad 1\leq\frac{\Delta t}{n\,\epsilon}<1+\frac{1}{n}.$$

Then by the squeeze theorem,

$$\lim_{\Delta t\to 0}\epsilon(n,\Delta t)=0 \text{ for any positive integer } n, \text{ and } \lim_{n\to\infty}\frac{\Delta t}{n\,\epsilon(n,\Delta t)}=1 \text{ for any } \Delta t>0. \quad \cdots(*2)$$

For such Δt, n and $\epsilon(n,\Delta t)$, $V_\epsilon(t_0+\Delta t)$ is bounded, since local extrema can occur only at which drugs switch by Proposition A.2. That is,

$$\begin{aligned}&\min\left[V_\epsilon(t_0+n\,\epsilon),V_\epsilon(t_0+(n+f)\epsilon),V_\epsilon(t_0+(n+1)\epsilon)\right]\ \le\ V_\epsilon(t_0+\Delta t)\\ &\le\ \max\left[V_\epsilon(t_0+n\,\epsilon),V_\epsilon(t_0+(n+f)\epsilon),V_\epsilon(t_0+(n+1)\epsilon)\right],\qquad\cdots(*3)\end{aligned}$$

Also,

$$\begin{aligned}&\lim_{\Delta t\to 0}\frac{\lim_{n\to\infty}V_{\epsilon(n,\Delta t)}(t_0+n\,\epsilon(n,\Delta t))-V(t_0)}{\Delta t}\\ =&\lim_{\Delta t\to 0}\lim_{n\to\infty}\frac{(\mathbb{B}_\epsilon\mathbb{A}_\epsilon)^n-I_2}{\Delta t}V(t_0) && \text{(by (*1))}\\ =&\frac{\lim_{\Delta t\to 0}\lim_{n\to\infty}\left[(\mathbb{B}_\epsilon\mathbb{A}_\epsilon)^n-I_2\right]/(n\,\epsilon)}{\lim_{\Delta t\to 0}\lim_{n\to\infty}\Delta t/(n\,\epsilon)}V(t_0)\\ =&\frac{\lim_{n\to\infty}\left[\lim_{\Delta t\to 0}\left[(\mathbb{B}_\epsilon\mathbb{A}_\epsilon)^n-I_2\right]/(n\,\epsilon)\right]}{\lim_{\Delta t\to 0}\left[\lim_{n\to\infty}\Delta t/(n\,\epsilon)\right]}V(t_0)\\ =&\frac{\lim_{n\to\infty}\left[\lim_{\epsilon\to 0}\left[(\mathbb{B}_\epsilon\mathbb{A}_\epsilon)^n-I_2\right]/(n\,\epsilon)\right]}{\lim_{\Delta t\to 0}1}V(t_0) && \text{by (*2)}\\ =&\lim_{n\to\infty}\left[f\,\mathbb{D}_A+(1-f)\mathbb{D}_B\right]V(t_0) && \text{(by Lemma A.6)}\\ =&(f\,\mathbb{D}_A+(1-f)\mathbb{D}_B)V(t_0). && \cdots(*4)\end{aligned}$$

And,

$$\begin{aligned}&\lim_{\Delta t\to 0}\frac{\lim_{n\to\infty}V_{\epsilon(n,\Delta t)}(t_0+(n+f)\,\epsilon(n,\Delta t))-V(t_0)}{\Delta t}\\ =&\lim_{\Delta t\to 0}\lim_{n\to\infty}\frac{\mathbb{A}_\epsilon(\mathbb{B}_\epsilon\mathbb{A}_\epsilon)^n-I_2}{\Delta t}V(t_0) && \text{(by (*1))}\\ =&\frac{\lim_{\Delta t\to 0}\lim_{n\to\infty}\left[\mathbb{A}_\epsilon(\mathbb{B}_\epsilon\mathbb{A}_\epsilon)^n-I_2\right]/((n+f)\,\epsilon)}{\lim_{\Delta t\to 0}\lim_{n\to\infty}\Delta t/((n+f)\,\epsilon)}V(t_0)\\ =&\frac{\lim_{n\to\infty}\left[\lim_{\Delta t\to 0}\left[(\mathbb{B}_\epsilon\mathbb{A}_\epsilon)^n-I_2\right]/((n+f)\,\epsilon)\right]}{\lim_{\Delta t\to 0}\left[\lim_{n\to\infty}(\Delta t/(n\,\epsilon))(n/(n+f))\right]}V(t_0)\\ =&\frac{\lim_{n\to\infty}\left[\lim_{\epsilon\to 0}\left[(\mathbb{B}_\epsilon\mathbb{A}_\epsilon)^n-I_2\right]/((n+f)\,\epsilon)\right]}{\lim_{\Delta t\to 0}1}V(t_0) && \text{by (*2)}\\ =&\lim_{n\to\infty}\left[\frac{(n+1)f}{n+f}\,\mathbb{D}_A+\frac{n(1-f)}{n+f}\mathbb{D}_B\right]V(t_0) && \text{(by Lemma A.7)}\\ =&(f\,\mathbb{D}_A+(1-f)\mathbb{D}_B)V(t_0) && \cdots(*5)\end{aligned}$$

Similar to (*4),

$$\lim_{\Delta t\to 0}\frac{\lim_{n\to\infty}V_{\epsilon(n,\Delta t)}(t_0+(n+1)\,\epsilon(n,\Delta t))-V(t_0)}{\Delta t}=(f\,\mathbb{D}_A+(1-f)\mathbb{D}_B)V(t_0)\quad\cdots(*6)$$

By (*4) - (*6),

$$\min\left[\lim_{\Delta t\to 0}\frac{\lim_{n\to\infty} V_\epsilon(t_0+n\,\epsilon)-V(t_0)}{\Delta t},\ \lim_{\Delta t\to 0}\frac{\lim_{n\to\infty} V_\epsilon(t_0+(n+f)\,\epsilon)-V(t_0)}{\Delta t},\right.$$
$$\left.\lim_{\Delta t\to 0}\frac{\lim_{n\to\infty} V_\epsilon(t_0+(n+1)\,\epsilon)-V(t_0)}{\Delta t}\right]=\max\left[\lim_{\Delta t\to 0}\frac{\lim_{n\to\infty} V_\epsilon(t_0+n\,\epsilon)-V(t_0)}{\Delta t},\right.$$
$$\left.\lim_{\Delta t\to 0}\lim_{\Delta t\to 0}\frac{\lim_{n\to\infty} V_\epsilon(t_0+(n+f)\,\epsilon)-V(t_0)}{\Delta t},\ \lim_{\Delta t\to 0}\frac{\lim_{n\to\infty} V_\epsilon(t_0+(n+1)\,\epsilon)-V(t_0)}{\Delta t}\right]$$
$$=(f\,\mathbb{D}_A+(1-f)\mathbb{D}_B)V(t_0) \qquad \cdots(*7)$$

Then, by (*3), (*7) and the squeeze theorem,

$$\left.\frac{d}{dt}V_0\right|_{t=t_0}=\lim_{\Delta t\to 0}\frac{\lim_{n\to\infty} V_\epsilon(t_0+\Delta t)-V(t_0)}{\Delta t}=(f\,\mathbb{D}_A+(1-f)\mathbb{D}_B)V(t_0)$$

Therefore,

$$\frac{dV}{dt}=(f\,\mathbb{D}_A+(1-f)\mathbb{D}_B)V$$

□

A.2 Population dynamics with the optimal regimen

Lemma A.9. $\left\{\dfrac{r_A r_B-s_A s_B}{r_A+r_B-s_A-s_B},\begin{pmatrix} ApB^* \\ 1\end{pmatrix}\right\}$ *is an eigen pair of* $f^*\,\mathbb{D}_A+(1-f^*)\mathbb{D}_B$ *with* ApB^* *and* f^* *from (8), (10) and (13).*

Proof. Let $\mathbb{D}^*:=f^*\,\mathbb{D}_A+(1-f^*)\mathbb{D}_B$, and $\lambda=\dfrac{r_A r_B-s_A s_B}{r_A+r_B-s_A-s_B}$. Then,

$$\mathbb{D}^*-\lambda\,I_2=C_1\begin{pmatrix} C_2\,U^T \\ C_3\,U^T\end{pmatrix},$$

where $U=\begin{pmatrix}1\\ -ApB^*\end{pmatrix}$ along with

$$C_1=-(g_A(r_A-s_B)+g_B(r_B-s_A)+(r_B-s_A)(r_A-s_B))(r_A+r_B-s_A-s_B)/(r_A-s_B),$$
$$C_2=g_A((r_A-s_B)(r_B-s_B)+g_B(r_A+r_B-s_A-s_B),$$
$$C_3=-g_B((r_B-s_A)(r_A-s_A)+g_A(r_A+r_B-s_A-s_B)).$$

Since $U^T\,V=0$ where $V=((r_B-s_A)/(r_A-s_B),1)^T$, (λ,V) is an eigen pair of $\mathbb{D}^*$. □

Theorem A.10. *In Stage 2 of the optimal strategy, both* A_R *and* B_R *changes with a constant net-proliferation rate,*

$$\lambda=\frac{r_A r_B-s_A s_B}{r_A+r_B-s_A-s_B}.$$

Proof. Without loss of generosity, let us prove it only when $ApB(0)<ApB^*$.

If $ApB(0) < ApB^*$, $DrugA$ has a better effect initially. So following the optimal therapy scheduling, $DrugA$ is assigned alone at the beginning as long as $T^A_{min} = T_{min}(p_A, p_B, ApB(0))$ (Stage 1), and then Stage 2 starts at T^A_{min} with initial condition

$$V(T^A_{min}) = \mathbb{M}_A(T^A_{min})V(0) = C \begin{pmatrix} ApB^* \\ 1 \end{pmatrix} \qquad \cdots (*1)$$

where $C = \dfrac{P(0)}{1+ApB(0)} \left(\dfrac{(r_A - s_A)(r_B - s_A) + g_A(r_A + r_B - s_A - s_B)}{(r_A - s_B)(g_A + ApB(0)(g_A + r_A - s_A))} \right)^{-\frac{g_A - s_A}{g_A + r_A - s_A}}$.

By Theorem A.8, in Stage 2, $V(t)$ obeys

$$\frac{dV}{dt} = \mathbb{D}^* V, \text{ where } \mathbb{D}^* = f^* \mathbb{D}_A + (1 - f^*)\mathbb{D}_B \qquad \cdots (*2)$$

By Lemma A.9, $V(T^A_{min})$ is an eigenvector of $\mathbb{D}^*$ with the corresponding eigenvalue, λ. Then, the solution of (*2) with the initial value (*1) is

$$V(t + T^A_{min}) = e^{\lambda\, t} V(T^A_{min}).$$

□

Theorem A.11. *With optimal therapy utilizing $DrugA$ and $DrugB$, V obeys the following equations and solutions.*

If $ApB(0) < ApB^*$,

$$\frac{dV}{dt} = \begin{cases} \mathbb{D}_A V & \text{if } 0 \le t \le T^A_{min} \\ \lambda\, V & \text{if } t > T^A_{min} \end{cases} \text{ and } V(t) = \begin{cases} \mathbb{M}_A(t)V(0) & \text{if } 0 \le t \le T^A_{min} \\ e^{\lambda\,(t - T^A_{min})} V(T^A_{min}) & \text{if } t > T^A_{min} \end{cases}$$

Similarly if $ApB(0) \ge ApB^*$,

$$\frac{dV}{dt} = \begin{cases} \mathbb{D}_B V & \text{if } 0 \le t \le T^B_{min} \\ \lambda\, V & \text{if } t > T^B_{min} \end{cases} \text{ and } V(t) = \begin{cases} \mathbb{M}_B(t)V(0) & \text{if } 0 \le t \le T^B_{min} \\ e^{\lambda\,(t - T^B_{min})} V(T^B_{min}) & \text{if } t > T^B_{min} \end{cases}$$

Proof. Straightforward, by Theorem A.10 □

Appendix B Sensitivity analysis on optimal scheduling

The two determinant quantities of optimal control scheduling are (i) the duration of the first stage (T^1_{min}), and (ii) the relative intensity between two drugs in the second stage (k^* or f^*). Here, we show sensitivity analysis on the quantities related to them over a range of model parameters.

Using g_1, we non-dimentionalize all the values, like

$$\{\overline{s_1}, \overline{r_1} | \overline{s_2}, \overline{r_2}\} := \frac{1}{g_1}\{s_1, r_1 | s_2, r_2\} \qquad \text{and} \qquad \overline{T_{gap}} := g_1\, T_{gap}$$

then,

$$\overline{T_{gap}}(\{\overline{s_1}, \overline{r_1}\}, \{\overline{s_2}, \overline{r_2}\}) := \frac{\ln\left[\dfrac{(1 - \overline{s_1})(\overline{r_1} - \overline{s_1})(\overline{r_1} - \overline{s_2})}{\overline{r_1}((\overline{r_1} - \overline{s_1})(\overline{r_2} - \overline{s_1}) + (\overline{r_1} + \overline{r_2} - \overline{s_1} - \overline{s_2}))}\right]}{1 + \overline{r_1} - \overline{s_1}} \qquad (11)$$

In general, cells mutate in a slower way than they proliferate **(ref)**, so we ran sensitivity analysis on T_{gap} for all $a \gg 1$ for $a \in \{-\overline{s_1}, -\overline{s_2}, \overline{r_1}, \overline{r_2}\}$. Figure 14 shows T_{gap} over the range of $20 \leq -\overline{s_1}, -\overline{s_2}, \overline{r_1}, \overline{r_2} \leq 100$. So, under the assumption that $g_1 \ll \min\{-s_1, -s_2, r_1, r_2\}$,

$$T_{gap}(\{s_1, r_1\}, \{s_2, r_2\}) \approx \frac{\ln\left[\dfrac{-s_1(r_1 - s_2)}{r_1(r_2 - s_1)}\right]}{r_1 - s_1},$$

which approximate the contour curves of Figure 14.

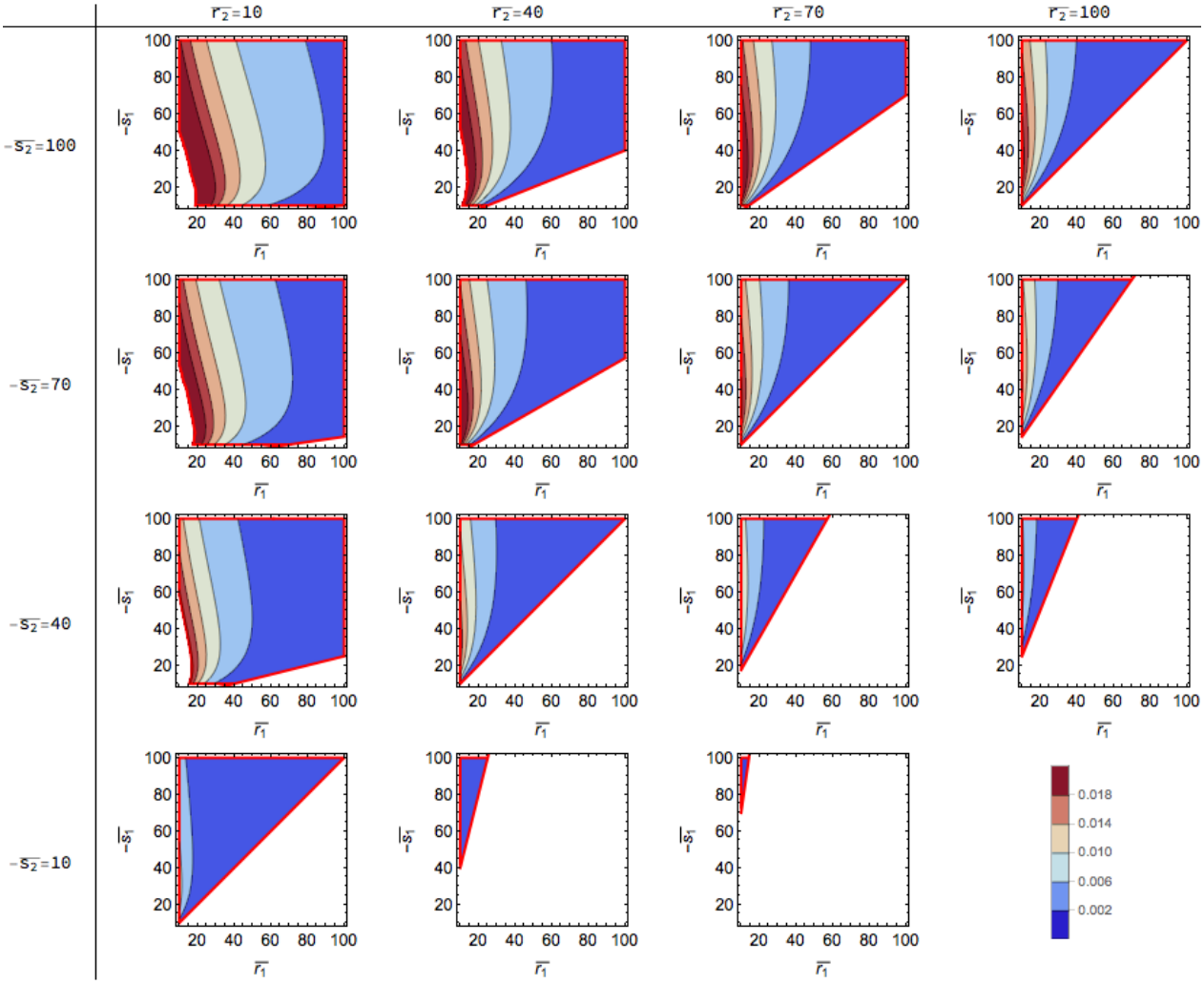

Figure 14: Contour maps of T_{gap} over ranges of $20 \leq a \leq 100$ for $a \in \{-s_1, -s_2, r_1, r_2\}$ and $r_1 r_2 < s_1 s_2$ (Condition (6))

Regarding the regulated intensities among the two drugs, k^*, we assumed that $g_1 \approx g_2 := g$, similarly assuming that they are both much smaller than $\{-s_1, -s_2, r_1, r_2\}$. Then we normalized all the parameters with the unit of g, like

$$\{\overline{s_1}, \overline{r_1} | \overline{s_2}, \overline{r_2}\} := \frac{1}{g}\{s_1, r_1 | s_2, r_2\}.$$

k^* can be rewritten in terms of the dimensionless parameters.

$$k^*(\{\overline{s_1},\overline{r_1}\},\{\overline{s_2},\overline{r_2}\}) = \frac{(\overline{r_1}-\overline{s_2})((\overline{r_1}-\overline{s_1})(\overline{r_2}-\overline{s_1})+(\overline{r_1}+\overline{r_2}-\overline{s_1}-\overline{s_2}))}{(\overline{r_2}-\overline{s_1})((\overline{r_2}-\overline{s_2})(\overline{r_1}-\overline{s_2})+(\overline{r_1}+\overline{r_2}-\overline{s_1}-\overline{s_2}))} \tag{12}$$

In sensitivity analysis, we use

$$f^* := \frac{k^*}{1+k^*}, \tag{13}$$

which represents intensity fraction of initially better drug out of total therapy. We evaluated f^* over the same ranges of $\{s_1, s_2, r_1, r_2\}$ like the previous exercise. (see Figure 15) Over the ranges, $\max\{g_1, g_2\} \ll \min\{-s_1, -s_2, r_1, r_2\}$, so k^* and f^* can be approximated by simpler forms.

$$k^* \approx \frac{r_1 - s_1}{r_2 - s_2} \qquad \text{and} \qquad f^* \approx \frac{r_1 - s_1}{r_1 + r_2 - s_1 - s_2}$$

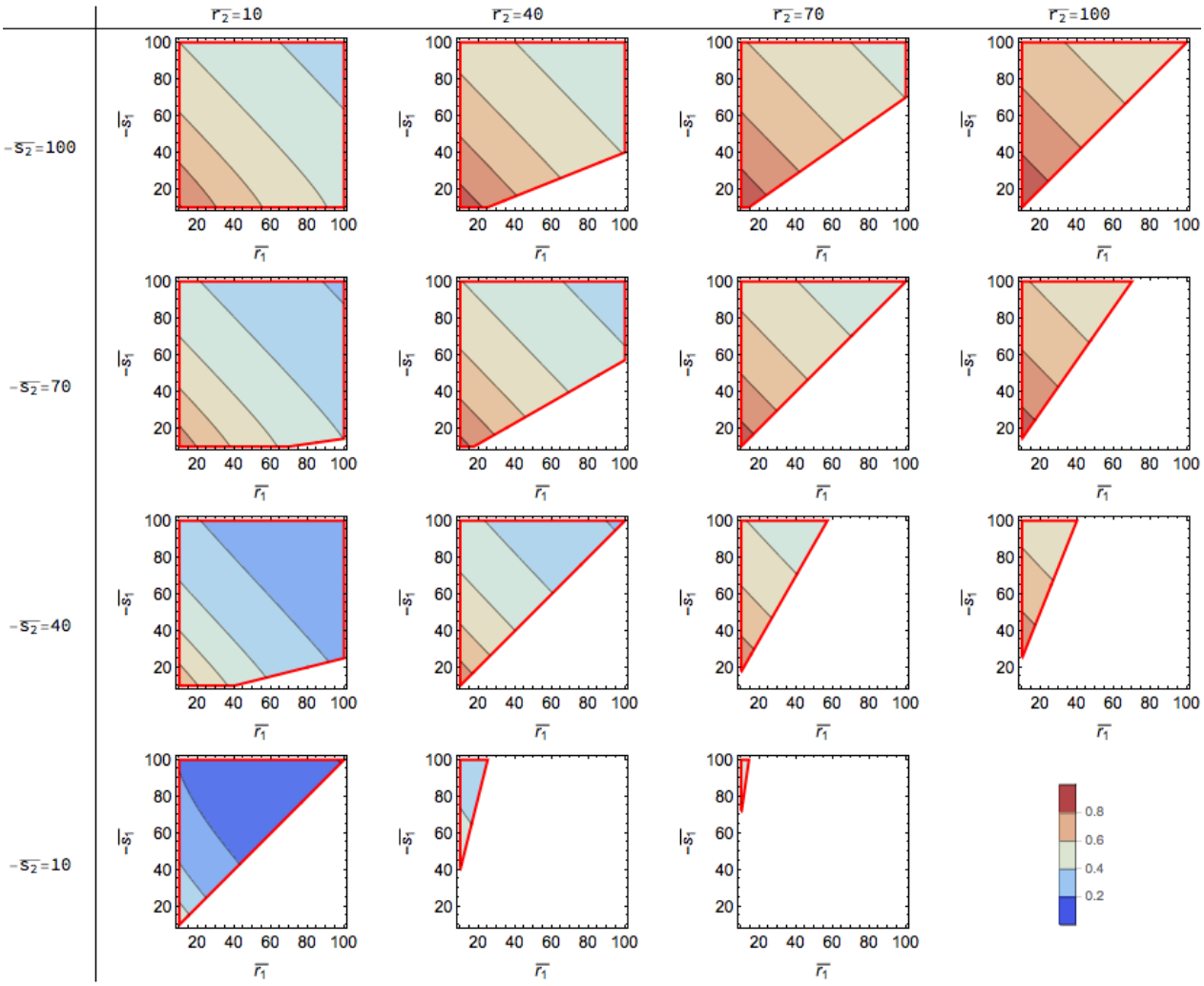

Figure 15: Contour maps of f^* over ranges of $20 \le a \le 100$ for $a \in \{-s_1, -s_2, r_1, r_2\}$ and $r_1 r_2 < s_1 s_2$ (Condition (6))

Appendix C Clinical implementation of instantaneous switch in the optimal strategy

In clinical practice, the instantaneous drug-switch which is proposed in this research to apply in the second stage of the optimal control is not implementable. Therefore, we studied similar schedules to the optimal case, and compared the therapy effects between the different schedules of administrations. In the "similar" schedules, the first stage with an initial drug remained same to the optimal schedule, but the second part of instantaneous switch (with $\Delta t = 0$) has been modified into fast switch ($\Delta t \gtrsim 0$). Figure 16 shows how the effect on population with instantaneous switch ($\Delta t = 0$)and fast switches (multiple choices of $\Delta t \gtrsim 0$) are different for a choice of drug parameter values. Expectedly, the smaller Δt is chosen, the closer to the ideal case of therapy effect. And, a choice of reasonably small Δt (like 1 day or 3 days) results in the outcome quite close to the optimal scenario.

We simulated same exercise with k^* (from (10)) instead of $k(\Delta t)$ modulated by Δt (Figure 17). Only invisibly small differences has been observed between Figure 16 and Figure 17, which justifies general usage of k^* independent from Δt.

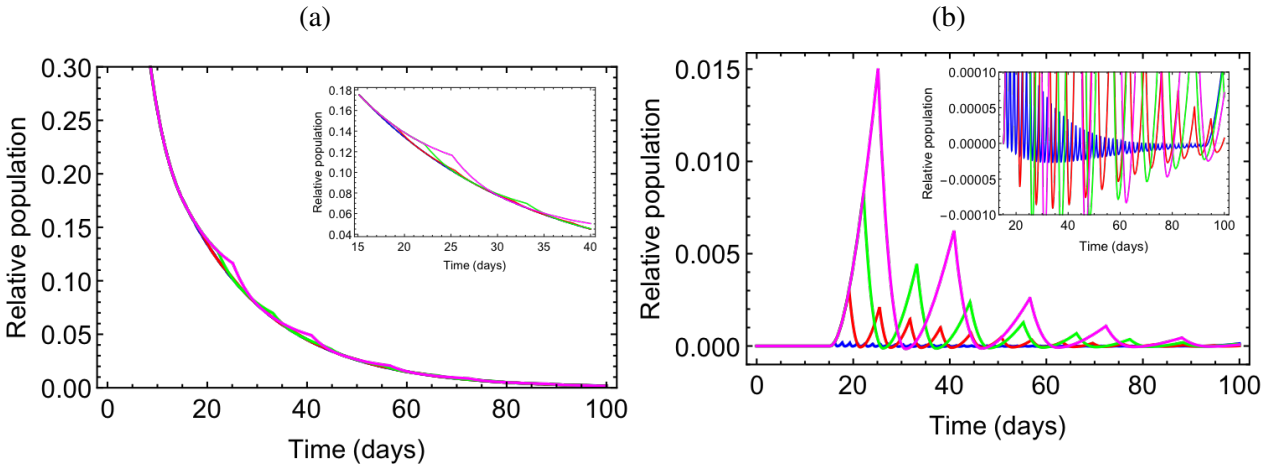

Figure 16: Graphs of regular drug switch in Stage 2 with different $\{\Delta t, k(\Delta t, p_A, p_B)\}$: $\Delta t = 1$ day (blue), $\Delta t = 4$ days (red), $\Delta t = 7$ days (green), and $\Delta t = 10$ days (magenta). Parameters/conditions: $p_A = \{-0.18, 0.008, 0.00075\}$/day, $p_B = \{-0.9, 0.016, 0.00125\}$/day and $\{A_R^0, B_R^0\} = \{0.1, 0.9\}$ (a) Time histories of total populations, C_P^n for $n \in \{1, 4, 7, 10\}$ days (b) Differences between the optimal population history C_P^*, (i.e., when $\Delta t = 0$) and each cases with positive Δt. (i.e., $C_P^n - C_P^*$). The inside smaller plots are same types of graphs with the bigger graphs, and show enlargement of interesting ranges.

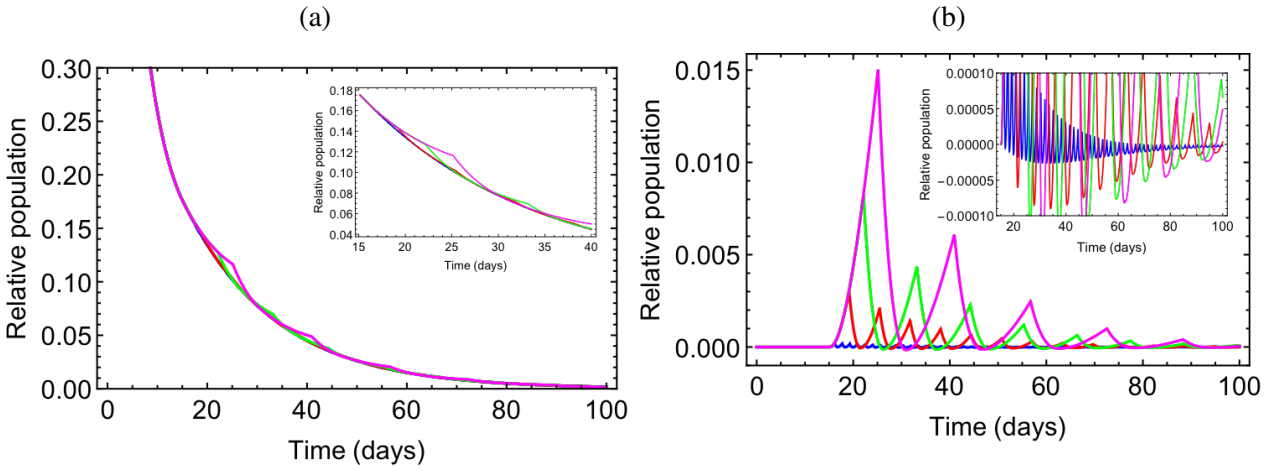

Figure 17: Graphs of regular drug switch in Stage 2 with different $\{\Delta t\}$ and fixed k^* from 10: $\Delta t = 1$ day (blue), $\Delta t = 4$ days (red), $\Delta t = 7$ days (green), and $\Delta t = 10$ days (magenta). Parameters/conditions: $p_A = \{-0.18, 0.008, 0.00075\}$/day, $p_B = \{-0.9, 0.016, 0.00125\}$/day and $\{A_R^0, B_R^0\} = \{0.1, 0.9\}$ (a) Time histories of total populations, C_P^n for $n \in \{1, 4, 7, 10\}$ days (b) Differences between the optimal population history C_P^*, (i.e., when $\Delta t = 0$) and each cases with positive Δt. (i.e., $C_P^n - C_P^*$). The inside smaller plots are same types of graphs with the bigger graphs, and show enlargement of interesting ranges.

Appendix D Stochastic simulation codes

The computational code written in Python will be provided at *Github* (https://github.com/nryoon12/Optimal-Therapy-Scheduling-Based-on-a-Pair-of-Collaterally-Sensitive-Drugs).